18. Gustafsson, B.E.; Karlsson, K.A.; Larson, G.; Midtvedt, T.; Stromberg, N.; Teneberg, S.; Thurin, J. Glycosphingolipid patterns of the gastrointestinal tract and feces of germ-free and conventional rats. *J. Biol. Chem.* **1986**, *261*, 15294–15300.
19. Vesper, H.; Schmelz, E.M.; Nikolova-Karakashian, M.N.; Dillehay, D.L.; Lynch, D.V.; Merrill, A.H., Jr. Sphingolipids in food and the emerging importance of sphingolipids to nutrition. *J. Nutr.* **1999**, *129*, 1239–1250.
20. Nilsson, A. Metabolism of sphingomyelin in the intestinal tract of the rat. *Biochim. Biophys. Acta* **1968**, *164*, 575–584.
21. Schmelz, E.M.; Crall, K.J.; Larocque, R.; Dillehay, D.L.; Merrill, A.H., Jr. Uptake and metabolism of sphingolipids in isolated intestinal loops of mice. *J. Nutr.* **1994**, *124*, 702–712.
22. Nilsson, A.; Duan, R.D. Alkaline sphingomyelinases and ceramidases of the gastrointestinal tract. *Chem. Phys. Lipids* **1999**, *102*, 97–105.
23. Tani, M.; Ito, M.; Igarashi, Y. Ceramide/sphingosine/sphingosine 1-phosphate metabolism on the cell surface and in the extracellular space. *Cell. Signal.* **2007**, *19*, 229–237.
24. Duan, R.D.; Nilsson, A. Metabolism of sphingolipids in the gut and its relation to inflammation and cancer development. *Prog. Lipid Res.* **2009**, *48*, 62–72.
25. Mazzei, J.C.; Zhou, H.; Brayfield, B.P.; Hontecillas, R.; Bassaganya-Riera, J.; Schmelz, E.M. Suppression of intestinal inflammation and inflammation-driven colon cancer in mice by dietary sphingomyelin: Importance of peroxisome proliferator-activated receptor gamma expression. *J. Nutr. Biochem.* **2011**, *22*, 1160–1171.
26. Fischbeck, A.; Leucht, K.; Frey-Wagner, I.; Bentz, S.; Pesch, T.; Kellermeier, S.; Krebs, M.; Fried, M.; Rogler, G.; Hausmann, M.; *et al.* Sphingomyelin induces cathepsin D-mediated apoptosis in intestinal epithelial cells and increases inflammation in DSS colitis. *Gut* **2011**, *60*, 55–65.
27. Sjoqvist, U.; Hertervig, E.; Nilsson, A.; Duan, R.D.; Ost, A.; Tribukait, B.; Lofberg, R. Chronic colitis is associated with a reduction of mucosal alkaline sphingomyelinase activity. *Inflamm. Bowel Dis.* **2002**, *8*, 258–263.
28. Maines, L.W.; Fitzpatrick, L.R.; French, K.J.; Zhuang, Y.; Xia, Z.; Keller, S.N.; Upson, J.J.; Smith, C.D. Suppression of ulcerative colitis in mice by orally available inhibitors of sphingosine kinase. *Dig. Dis. Sci.* **2008**, *53*, 997–1012.
29. Nyberg, L.; Duan, R.D.; Nilsson, A. A mutual inhibitory effect on absorption of sphingomyelin and cholesterol. *J. Nutr. Biochem.* **2000**, *11*, 244–249.
30. Allende, M.L.; Bektas, M.; Lee, B.G.; Bonifacino, E.; Kang, J.; Tuymetova, G.; Chen, W.; Saba, J.D.; Proia, R.L. Sphingosine-1-phosphate lyase deficiency produces a pro-inflammatory response while impairing neutrophil trafficking. *J. Biol. Chem.* **2011**, *286*, 7348–7358.
31. Bagdanoff, J.T.; Donoviel, M.S.; Nouraldeen, A.; Tarver, J.; Fu, Q.; Carlsen, M.; Jessop, T.C.; Zhang, H.; Hazelwood, J.; Nguyen, H.; *et al.* Inhibition of sphingosine-1-phosphate lyase for the treatment of autoimmune disorders. *J. Med. Chem.* **2009**, *52*, 3941–3953.
32. Bandhuvula, P.; Honbo, N.; Wang, G.Y.; Jin, Z.Q.; Fyrst, H.; Zhang, M.; Borowsky, A.D.; Dillard, L.; Karliner, J.S.; Saba, J.D. S1p lyase: A novel therapeutic target for ischemia-reperfusion injury of the heart. *Am. J. Physiol. Heart Circ. Physiol.* **2011**, *300*, H1753–H1761.

33. Kunisawa, J.; McGhee, J.; Kiyono, H. Mucosal S-IgA Enhancement: Development of Safe and Effective Mucosal Adjuvants and Mucosal Antigen Delivery Vehicles. In *Mucosal Immune Defense: Immunoglobulin A*; Kaetzel, C., Ed.; Kluwer Academic/Plenum Publishers: New York, NY, USA, 2007; pp. 346–389.
34. Fagarasan, S.; Kawamoto, S.; Kanagawa, O.; Suzuki, K. Adaptive immune regulation in the gut: T cell-dependent and T cell-independent IgA synthesis. *Annu. Rev. Immunol.* **2010**, *28*, 243–273.
35. Kunisawa, J.; Nochi, T.; Kiyono, H. Immunological commonalities and distinctions between airway and digestive immunity. *Trends Immunol.* **2008**, *29*, 505–513.
36. Neutra, M.R.; Mantis, N.J.; Kraehenbuhl, J.P. Collaboration of epithelial cells with organized mucosal lymphoid tissues. *Nat. Immunol.* **2001**, *2*, 1004–1009.
37. Gohda, M.; Kunisawa, J.; Miura, F.; Kagiyama, Y.; Kurashima, Y.; Higuchi, M.; Ishikawa, I.; Ogahara, I.; Kiyono, H. Sphingosine 1-phosphate regulates the egress of IgA plasmablasts from Peyer's patches for intestinal IgA responses. *J. Immunol.* **2008**, *180*, 5335–5343.
38. Graler, M.H.; Goetzl, E.J. The immunosuppressant FTY720 down-regulates sphingosine 1-phosphate G-protein-coupled receptors. *FASEB J.* **2004**, *18*, 551–553.
39. Kunisawa, J.; Kiyono, H. A marvel of mucosal T cells and secretory antibodies for the creation of first lines of defense. *Cell Mol. Life Sci.* **2005**, *62*, 1308–1321.
40. Kunisawa, J.; Kurashima, Y.; Gohda, M.; Higuchi, M.; Ishikawa, I.; Miura, F.; Ogahara, I.; Kiyono, H. Sphingosine 1-phosphate regulates peritoneal B-cell trafficking for subsequent intestinal IgA production. *Blood* **2007**, *109*, 3749–3756.
41. Kunisawa, J.; Gohda, M.; Kurashima, Y.; Ishikawa, I.; Higuchi, M.; Kiyono, H. Sphingosine 1-phosphate-dependent trafficking of peritoneal B cells requires functional NFκB-inducing kinase in stromal cells. *Blood* **2008**, *111*, 4646–4652.
42. Kunisawa, J.; Takahashi, I.; Kiyono, H. Intraepithelial lymphocytes: Their shared and divergent immunological behaviors in the small and large intestine. *Immunol. Rev.* **2007**, *215*, 136–153.
43. Vivier, E.; Tomasello, E.; Paul, P. Lymphocyte activation via NKG2D: Towards a new paradigm in immune recognition? *Curr. Opin. Immunol.* **2002**, *14*, 306–311.
44. Natarajan, K.; Dimasi, N.; Wang, J.; Mariuzza, R.A.; Margulies, D.H. Structure and function of natural killer cell receptors: Multiple molecular solutions to self, nonself discrimination. *Annu. Rev. Immunol.* **2002**, *20*, 853–885.
45. Gangadharan, D.; Lambolez, F.; Attinger, A.; Wang-Zhu, Y.; Sullivan, B.A.; Cheroutre, H. Identification of pre- and postselection TCRαβ$^+$ intraepithelial lymphocyte precursors in the thymus. *Immunity* **2006**, *25*, 631–641.
46. Kunisawa, J.; Kurashima, Y.; Higuchi, M.; Gohda, M.; Ishikawa, I.; Ogahara, I.; Kim, N.; Shimizu, M.; Kiyono, H. Sphingosine 1-phosphate dependence in the regulation of lymphocyte trafficking to the gut epithelium. *J. Exp. Med.* **2007**, *204*, 2335–2348.
47. Sharma, S.; Mathur, A.G.; Pradhan, S.; Singh, D.B.; Gupta, S. Fingolimod (FTY720): First approved oral therapy for multiple sclerosis. *J. Pharmacol. Pharmacother.* **2011**, *2*, 49–51.
48. Kweon, M.N.; Yamamoto, M.; Kajiki, M.; Takahashi, I.; Kiyono, H. Systemically derived large intestinal CD4$^+$ Th2 cells play a central role in STAT6-mediated allergic diarrhea. *J. Clin. Invest.* **2000**, *106*, 199–206.

49. Kurashima, Y.; Kunisawa, J.; Higuchi, M.; Gohda, M.; Ishikawa, I.; Takayama, N.; Shimizu, M.; Kiyono, H. Sphingosine 1-phosphate-mediated trafficking of pathogenic Th2 and mast cells for the control of food allergy. *J. Immunol.* **2007**, *179*, 1577–1585.
50. Gurish, M.F.; Boyce, J.A. Mast cell growth, differentiation, and death. *Clin. Rev. Allergy Immunol.* **2002**, *22*, 107–118.
51. Mizushima, T.; Ito, T.; Kishi, D.; Kai, Y.; Tamagawa, H.; Nezu, R.; Kiyono, H.; Matsuda, H. Therapeutic effects of a new lymphocyte homing reagent FTY720 in interleukin-10 gene-deficient mice with colitis. *Inflamm. Bowel Dis.* **2004**, *10*, 182–192.
52. Fujii, R.; Kanai, T.; Nemoto, Y.; Makita, S.; Oshima, S.; Okamoto, R.; Tsuchiya, K.; Totsuka, T.; Watanabe, M. FTY720 suppresses $CD4^{+}$ $CD44^{high}$ $CD62L^{-}$ effector memory T cell-mediated colitis. *Am. J. Physiol. Gastrointest. Liver Physiol.* **2006**, *291*, G267–G274.
53. Deguchi, Y.; Andoh, A.; Yagi, Y.; Bamba, S.; Inatomi, O.; Tsujikawa, T.; Fujiyama, Y. The S1P receptor modulator FTY720 prevents the development of experimental colitis in mice. *Oncol. Rep.* **2006**, *16*, 699–703.

frontiers in IMMUNOLOGY

REVIEW ARTICLE
published: 02 April 2012
doi: 10.3389/fimmu.2012.00065

Alcaligenes is commensal bacteria habituating in the gut-associated lymphoid tissue for the regulation of intestinal IgA responses

Jun Kunisawa[1,2]* and Hiroshi Kiyono[1,2,3,4]*

[1] Division of Mucosal Immunology, Department of Microbiology and Immunology, Institute of Medical Science, The University of Tokyo, Tokyo, Japan
[2] Department of Medical Genome Science, Graduate School of Frontier Science, The University of Tokyo, Tokyo, Japan
[3] Graduate School of Medicine, The University of Tokyo, Tokyo, Japan
[4] Core Research for Evolutional Science and Technology, Japan Science and Technology Agency, Tokyo, Japan

Edited by:
Nils Yngve Lycke, University of Gothenburg, Sweden

Reviewed by:
Paul King, Monash University, Australia
Hiroshi Ohno, RIKEN, Japan

***Correspondence:**
Jun Kunisawa and Hiroshi Kiyono, Division of Mucosal Immunology, Department of Microbiology and Immunology, Institute of Medical Science, The University of Tokyo, Tokyo, Japan.
e-mail: kunisawa@ims.u-tokyo.ac.jp; kiyono@ims.u-tokyo.ac.jp

Secretory-immunoglobulin A (S-IgA) plays an important role in immunological defense in the intestine. It has been known for a long time that microbial stimulation is required for the development and maintenance of intestinal IgA production. Recent advances in genomic technology have made it possible to detect uncultivable commensal bacteria in the intestine and identify key bacteria in the regulation of innate and acquired mucosal immune responses. In this review, we focus on the immunological function of Peyer's patches (PPs), a major gut-associated lymphoid tissue, in the induction of intestinal IgA responses and the unique immunological interaction of PPs with commensal bacteria, especially *Alcaligenes*, a unique indigenous bacteria habituating inside PPs.

Keywords: Peyer's patch, IgA, commensal bacteria

INTRODUCTION

Secretory-immunoglobulin A (S-IgA) is predominantly observed in the intestine where it participates in immune defense (Mestecky et al., 2005; Brandtzaeg, 2010). S-IgA inhibits adherence of pathogens to host epithelial cells in the intestinal lumen and neutralizes pathogenic toxins by binding to the toxins' biologically active sites. Based on the immunological importance of S-IgA in immunosurveillance in the intestine, the development of oral vaccines has focused on the induction of antigen-specific S-IgA responses (Kunisawa et al., 2007). In addition to the immunosurveillance in the intestine, S-IgA antibody contributes to the establishment of beneficial gut commensal microbiota and thus dysfunction of S-IgA formation resulted in the alteration of normal bacterial flora (e.g., the reduction of Lactobacillus and increase of segmented filamentous bacteria, SFB; Suzuki et al., 2004).

Peyer's patches (PPs) are major gut-associated lymphoid tissue (GALT) where intestinal IgA responses are initiated and regulated by unique immunological crosstalk via cytokines [e.g., interleukin-4 (IL-4), IL-6, IL-21, and transforming growth factor-β (TGF-β)] and cell–cell interactions (e.g., via CD40/CD40 ligand interactions) among dendritic, T, and B cells (Kunisawa et al., 2008; Fagarasan et al., 2010). Thus, oral delivery of antigens to PPs is considered an important strategy for the effective induction of antigen-specific intestinal IgA responses (Kunisawa et al., 2011).

In addition to host-derived factors, microbial stimulation is also required for the maximum production of S-IgA in the intestine (Cebra et al., 2005). Indeed, germ-free (GF) mice have decreased intestinal IgA responses with immature structure of GALT when compared with mice housed under SPF or conventional conditions (Weinstein and Cebra, 1991). Although it was reported that some commensal bacteria [e.g., SFB and altered Schaedler flora (ASF), a combined eight culturable bacteria] and bacterial products (e.g., peptidoglycan, CpG oligonucleotide, and LPS) stimulated the intestinal IgA production (Michalek et al., 1983; Talham et al., 1999; Butler et al., 2005), it is obscure which bacteria is involved in this process indigenously. Because predominant commensal bacteria in the intestine is uncultivable, it was difficult to determine by culture-based method which bacteria regulated specific immune responses. However, recent advances in the genomic analysis allowed us to identify the uncultivable bacteria, which revealed key bacteria in the regulation of specific immune responses (Ivanov et al., 2009; Atarashi et al., 2011) as well as the development of immune diseases (Chow et al., 2010; Hill and Artis, 2010). Using genomic and immunological methods, we recently found that the microbial community inside PPs is different from those on the epithelium of PPs or in the intestinal lumen (Obata et al., 2010).

In this review, we discuss initially the immunological features of PPs in the induction and regulation of intestinal IgA responses. In the later part, we focus on the unique cross-communication between PPs and habitat commensal bacteria, *Alcaligenes*, a unique indigenous bacteria habituating inside PPs and regulating dendritic cells (DCs) for the efficient production of intestinal IgA.

IMMUNOLOGICAL FEATURES OF PEYER'S PATCHES

In the intestine, GALT comprise several different, organized lymphoid structures (Spencer et al., 2009; Fagarasan et al., 2010). Among them, PPs are the largest and most well-characterized sites

for the initiation of intestinal IgA responses, especially responses to T cell-dependent antigens (Kunisawa et al., 2008; Fagarasan et al., 2010). There are generally 8–10 PPs in the mouse small intestine and hundreds in the human small intestine. Each PP is composed of several B cell-rich follicles surrounded by a mesh-like structure consisting of T cells known as the interfollicular region (**Figure 1**).

Inside PPs, antigen-sampling M cells located in the follicle-associated epithelium transport luminal antigens to DCs situated in the subepithelium region (Neutra et al., 2001), which then form clusters with T-, B-, and stromal cells in the germinal centers and promote μ-to-α-class-switch recombination of B cells with the help of cytokines such as IL-4, IL-21, and TGF-β (Fagarasan et al., 2010). Upon immunoglobulin class-switching from μ to α, IgA-committed B cells (IgA^+ B cells) begin to express type 1 sphingosine-1-phosphate receptor, CCR9, and α4β7 integrin, allowing them to depart from the PPs and subsequently traffic to the intestinal lamina propria (Mora et al., 2006; Gohda et al., 2008). In the intestinal lamina propria, they further differentiate into IgA-secreting plasma cells under the influence of terminal differentiation factors (e.g., IL-6; Cerutti et al., 2011). DCs play a key role in these processes. For instance, nitric oxide, TGF-β, APRIL, and BAFF produced by TNF-α/iNOS-producing DCs (Tip-DCs) promotes IgA production (Tezuka et al., 2007). Also, DCs in the PPs metabolite vitamin A and produce retinoic acid, which induces the expression of gut-homing receptors (CCR9, and α4β7 integrin) on activated B and T cells (Iwata et al., 2004; Mora et al., 2006). Retinoic acid also induces the preferential differentiation into regulatory T (Treg) cells (Hall et al., 2011), and some of Treg cells differentiated into follicular helper T cells to promote IgA production in the PPs (Tsuji et al., 2009).

The identification of the molecular pathway of PP organogenesis allowed the establishment of PP-deficient mice through the loss of any part of this pathway (Nishikawa et al., 2003). Notably, disruption of the PP organogenesis pathway by blockade of tissue genesis cytokine receptor signaling [IL-7R and/or lymphotoxin-β receptor (LTβR)] during a limited fetus time period results in the selective loss of PPs without affecting other lymphoid tissue organogenesis (Yoshida et al., 1999). Experiments with PP-deficient mice showed that the dependency on PPs in the induction of antigen-specific IgA responses depends on the form of the antigen. For instance, the PP-deficient mice failed to develop antigen-specific IgA responses against orally administered antigens in particle form, but retained their ability to respond to soluble forms of antigens (Yamamoto et al., 2000; Kunisawa et al., 2002). It was also reported that lamina propria DCs are capable of initiating systemic IgG responses, whereas antigen transport by M cells into the PPs is required for the induction of intestinal IgA production (Martinoli et al., 2007). This is consistent with another finding that DCs in the PPs are responsible for intestinal IgA production (Fleeton et al., 2004). Therefore, PPs are considered to be one of the major sites for the initiation of intestinal antigen-specific IgA responses.

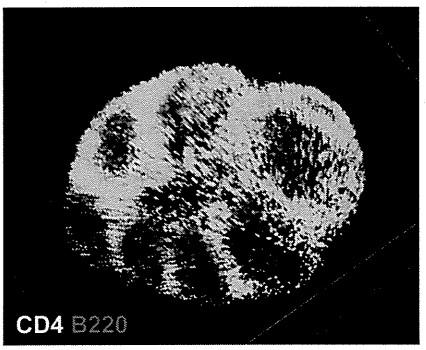

FIGURE 1 | Microarchitecture of murine Peyer's patches. Purified T cells (green) and B cells (red) were chemically labeled with carboxyfluorescein succinimidyl ester and carboxy-SNARF-1, respectively, and adoptively transferred into mice. Fifteen hours after the transfer, cell distribution in the Peyer's patches was observed at the whole-tissue level by using macro-confocal microscopy.

EFFECT OF MICROBIAL STIMULATION ON THE PRODUCTION OF INTESTINAL IgA

It is well known that microbial stimulation is required for the full production of S-IgA in the intestine. Indeed, GF mice have decreased intestinal IgA responses when compared with mice housed under SPF or conventional conditions (Cebra et al., 2005). Studies using mono-associated GF mice with SFB have demonstrated that only a minor proportion of the total intestinal IgA is reactive to mono-associated bacteria (Talham et al., 1999). In addition, bacterial products produced by commonly expressed on commensal bacteria (e.g., peptidoglycan, CpG oligonucleotide, and LPS) stimulated the intestinal IgA production (Michalek et al., 1983; Butler et al., 2005). In contrast, a recent study using reversible colonization of GF mice with genetically engineered *E. coli* showed that intestinal IgA induced in those mice bound to parent strain but not other bacteria (Hapfelmeier et al., 2010). Therefore, it remains unclear whether intestinal IgA responses induced by commensal bacteria is mediated by polyclonal stimulation and/or by B cell receptors specific for microbial antigens.

As one mechanism of impaired IgA production of GF mice, it was reported that GF mice have structurally immature GALT (e.g., PPs and ILFs) when compared with SPF mice (Weinstein and Cebra, 1991; Hamada et al., 2002). In the PPs, several key pathways for the IgA production require microbial stimulation. For example, Tip-DCs enhance the IgA production by producing nitric oxide, TGF-β, APRIL, and BAFF, which requires microbial stimulation through innate receptors (Tezuka et al., 2007). Indeed, the number of Tip-DCs was much reduced in the intestine of GF and MyD88-deficient mice (Tezuka et al., 2007). Another cell involved the microbe-dependent IgA production is non-hematopoietic follicular DCs (FDCs). It was reported that microbial stimulation of FDCs resulted in expressing chemokine CXCL13, BAFF, and TGF-β for the germinal center formation and B cell class-switching from IgM to IgA (Suzuki et al., 2010).

ALCALIGENES IS A UNIQUE INDIGENOUS BACTERIA INSIDE PPs

Recent advances in genomic technology make it possible to detect commensal bacteria in the intestine, allowing identification of key bacteria involved in the regulation of specific immune responses. For example, SFB was identified as commensal bacteria inducing

Th17 cells (Ivanov et al., 2009), whereas colonic regulatory T cells were induced by *Clostridium* clusters IV and XIV (Atarashi et al., 2011). These commensal bacteria localize at the surface of intestinal epithelium, but we supposed that the immunological crosstalk between host and commensal bacteria might establish in the regulation of intestinal IgA responses in the GALT. In this issue, we analyzed the composition of the microbial community inside PPs and identified *Alcaligenes* as a major commensal bacteria uniquely locating inside PPs (Obata et al., 2010).

By using the 16S rRNA clone library method, SFB are the predominant commensal bacteria co-habitat on FAE of PPs as like small intestinal epithelium. Although the FAE consisted with antigen-sampling M cells, SFB was not found inside of PPs. Instead, *Alcaligenes* are predominant bacteria inside PPs. The result obtained by the 16S rRNA analysis was further confirmed by fluorescence *in situ* hybridization (FISH) method and thus *Alcaligenes* are present exclusively inside PPs, not on the FAE of PPs, and intestinal villous epithelium and intestinal lamina propria (**Figure 2**). Of note, the preferential presence of *Alcaligenes* was observed not only in mouse but also in monkey and human (Obata et al., 2010). One of interesting but unresolved questions is the species specificity of *Alcaligenes*. We are now investigating whether *Alcaligenes* isolated from human or monkey colonize in the PPs to promote IgA production when they are orally fed to GF mice. Inside PPs, a proportion of the *Alcaligenes* seemed to be alive in mice. The presence and growth of *Alcaligenes* were detected in the PPs of GF mice after adoptive transfer of PP homogenates containing *Alcaligenes* from SPF mice. These findings suggest that *Alcaligenes* are indigenous bacteria ubiquitously living inside the PPs of various mammalian species.

ANTIBODY-MEDIATED RECIPROCAL INTERACTION BETWEEN *ALCALIGENES* AND THE HOST IMMUNE SYSTEM

As mentioned above, M cells located on the FAE of PPs transport luminal bacteria into DCs locating at the subepithelial region of FAE (Neutra et al., 2001). 16S rRNA clone library methods consistently revealed that DCs in the PPs predominantly contain *Alcaligenes*, whereas these bacteria are rarely detected in DCs isolated from other lymphoid tissues (e.g., spleen and mesenteric lymph nodes; Obata et al., 2010). We examined the immunological effects of *Alcaligenes* on DCs and found that the production of IgA-enhancing cytokines such as IL-6, TGF-β, and BAFF was increased when DCs isolated from the PPs of GF mice were stimulated with *Alcaligenes* (Obata et al., 2010). Several lines of evidence have revealed that immunological functions of DCs are different between intestinal and other lymphoid tissues (reviewed in Rescigno, 2010), we are now investigating whether immune stimulatory functions of *Alcaligenes* is specific for the PP DCs or not.

In agreement with the uptake of *Alcaligenes* and subsequent production of IgA-enhancing cytokines by DCs, *Alcaligenes*-specific IgA-forming cells were frequently observed in PPs, and consequent IgA production was noted in the intestinal lumen of SPF mice, but not GF mice (Obata et al., 2010). Although biological role of *Alcaligenes*-specific IgA antibody remains to be elucidated, the antibody might be involved in the creation of intratissue co-habitation of *Alcaligenes* in PPs. To this end, the number of *Alcaligenes* inside PPs is decreased in B cell-deficient CBA/N xid and IgA-deficient mice compared with wild-type mice (Obata et al., 2010). Therefore, it is interesting to suggest that *Alcaligenes*-specific IgA antibody mediates the uptake and presence of *Alcaligenes* in the PPs. Since M cells express IgA receptors

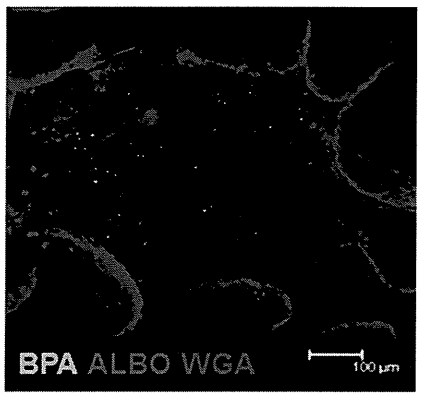

FIGURE 2 | Microarchitecture of murine Peyer's patches. Whole-mount fluorescence *in situ* hybridization was performed to visually analyze the presence of *Alcaligenes* inside PPs. Both BPA and ALBO34a were used as specific probes for *Alcaligenes*. Wheat germ agglutinin (WGA), an *N*-acetylglucosamine-specific lectin, was used to detect epithelial cells. Scale bar indicates 100 μm.

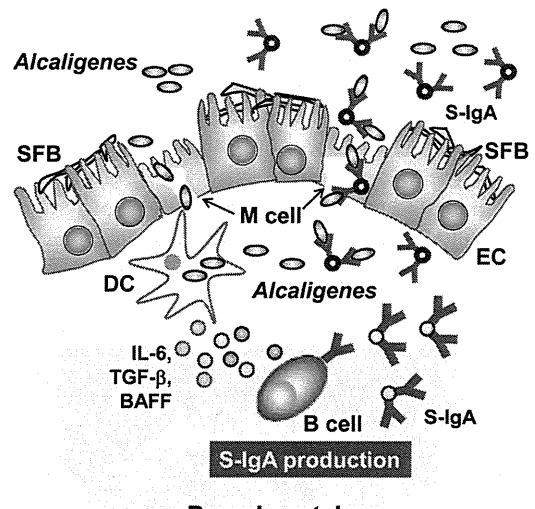

FIGURE 3 | *Alcaligenes* mediates symbiotic communication inside Peyer's patches. On the follicle-associated epithelium of PPs, segmented filamentous bacteria (SFB) is predominantly observed. In contrast, *Alcaligenes* specifically localizes inside Peyer's patches, where some are taken up by dendritic cells (DCs). Stimulation by *Alcaligenes* prompts the DCs to produce IgA-enhancing cytokines [e.g., interleukin-6 (IL-6), transforming growth factor-β (TGF-β)], and B cell activating factor (BAFF), which enhance the intestinal IgA response. The intestinal IgA includes *Alcaligenes*-specific IgA, which might mediate the preferential uptake and presence of *Alcaligenes* in the PPs. The uptake is presumably mediated by M cells.

(Mantis et al., 2002), one possibility is that *Alcaligenes* coated with the *Alcaligenes*-specific antibody are taken up into PPs through M cells. Further, the antigen-specific IgA coating on *Alcaligenes* might be beneficial for the bacteria to create the co-habitation niche since IgA antibody has been shown to non-inflammatory antibody (Mestecky et al., 2005).

CONCLUSION

In this review, we discussed a new concept of symbiotic communication in PPs that is mediated by commensal bacteria-specific IgA antibody. *Alcaligenes*-specific antibodies may mediate the uptake and the presence of *Alcaligenes* in the PPs, and the co-habitation of *Alcaligenes* within the PPs is one of the key factors to promote the intestinal IgA production by enhancing the production of IgA-enhancing cytokines from DCs (**Figure 3**). We still have various questions regarding this co-habitation of *Alcaligenes* in the PPs. For example, it remains unclear whether the presence of *Alcaligenes* inside of PPs is physiologically beneficial or harmful for the host immune system. In this issue, we are now addressing the microbial community in the PPs of mice and human patients suffering from intestinal immune diseases (e.g., intestinal inflammation and allergy). The biological roles of intra-tissue habitation of *Alcaligenes* in the PPs in the appropriate regulation of mucosal immune responses need to be elucidated. The current goal is to elucidate the mechanisms behind the co-habitation of *Alcaligenes* within PPs, and the exact contribution of *Alcaligenes* to educate and guide mucosal immunocompetent cells especially DCs in the PPs for the development, maturation and maintenance of the appropriate host immune system. These studies will provide novel molecular and cellular mechanisms of symbiotic communication with commensal bacteria in the regulation of host immunity.

ACKNOWLEDGMENTS

We thank Dr. T. Obata for his contribution to all works related to *Alcaligenes*, Drs. Y. Benno and M. Sakamoto (RIKEN BioResource Center), and Drs. Y. Umesaki, T. Matsuki, H. Setoyama (Yakult Central Institute for Microbiological Research) for their constructive discussions, technical advice, and supports on microbial analyses, and Dr. H. Iijima (Osaka University) for providing human samples. The work related to this review was supported by grants from the Ministry of Education, Culture, Sports, Science and Technology of Japan [Grant-in-Aid for Young Scientists A (22689015 to Jun Kunisawa), for Scientific Research on Innovative Areas (23116506 to Jun Kunisawa), for Scientific Research S (23229004 to Hiroshi Kiyono), and for Scientific Research on Priority Area (19059003 to Hiroshi Kiyono)]; the Ministry of Health and Welfare of Japan (to Jun Kunisawa and Hiroshi Kiyono); the Global Center of Excellence Program of the Center of Education and Research for Advanced Genome-based Medicine (to Hiroshi Kiyono); the Program for Promotion of Basic and Applied Researches for Innovations in Bio-oriented Industry (to Jun Kunisawa); and the Yakult Bio-Science Foundation (to Jun Kunisawa).

REFERENCES

Atarashi, K., Tanoue, T., Shima, T., Imaoka, A., Kuwahara, T., Momose, Y., Cheng, G., Yamasaki, S., Saito, T., Ohba, Y., Taniguchi, T., Takeda, K., Hori, S., Ivanov, I. I., Umesaki, Y., Itoh, K., and Honda, K. (2011). Induction of colonic regulatory T cells by indigenous *Clostridium* species. *Science* 331, 337–341.

Brandtzaeg, P. (2010). Function of mucosa-associated lymphoid tissue in antibody formation. *Immunol. Invest.* 39, 303–355.

Butler, J. E., Francis, D. H., Freeling, J., Weber, P., and Krieg, A. M. (2005). Antibody repertoire development in fetal and neonatal piglets. IX. Three pathogen-associated molecular patterns act synergistically to allow germfree piglets to respond to type 2 thymus-independent and thymus-dependent antigens. *J. Immunol.* 175, 6772–6785.

Cebra, J. J., Jiang, H. Q., Boiko, N. V., and Tlaskalva-Hogenova, H. (2005). "The role of mucosal microbiota in the development, maintenance, and pathologies of the mucosal immune system," in *Mucosal Immunology*, 3rd Edn, eds J. Mestecky, M. E. Lamm, W. Strober, J. Bienenstock, J. R. Mcghee, and L. Mayer (San Diego: Academic Press), 335–368.

Cerutti, A., Chen, K., and Chorny, A. (2011). Immunoglobulin responses at the mucosal interface. *Annu. Rev. Immunol.* 29, 273–293.

Chow, J., Lee, S. M., Shen, Y., Khosravi, A., and Mazmanian, S. K. (2010). Host-bacterial symbiosis in health and disease. *Adv. Immunol.* 107, 243–274.

Fagarasan, S., Kawamoto, S., Kanagawa, O., and Suzuki, K. (2010). Adaptive immune regulation in the gut: T cell-dependent and T cell-independent IgA synthesis. *Annu. Rev. Immunol.* 28, 243–273.

Fleeton, M. N., Contractor, N., Leon, F., Wetzel, J. D., Dermody, T. S., and Kelsall, B. L. (2004). Peyer's patch dendritic cells process viral antigen from apoptotic epithelial cells in the intestine of reovirus-infected mice. *J. Exp. Med.* 200, 235–245.

Gohda, M., Kunisawa, J., Miura, F., Kagiyama, Y., Kurashima, Y., Higuchi, M., Ishikawa, I., Ogahara, I., and Kiyono, H. (2008). Sphingosine 1-phosphate regulates the egress of IgA plasmablasts from Peyer's patches for intestinal IgA responses. *J. Immunol.* 180, 5335–5343.

Hall, J. A., Grainger, J. R., Spencer, S. P., and Belkaid, Y. (2011). The role of retinoic acid in tolerance and immunity. *Immunity* 35, 13–22.

Hamada, H., Hiroi, T., Nishiyama, Y., Takahashi, H., Masunaga, Y., Hachimura, S., Kaminogawa, S., Takahashi-Iwanaga, H., Iwanaga, T., Kiyono, H., Yamamoto, H., and Ishikawa, H. (2002). Identification of multiple isolated lymphoid follicles on the antimesenteric wall of the mouse small intestine. *J. Immunol.* 168, 57–64.

Hapfelmeier, S., Lawson, M. A., Slack, E., Kirundi, J. K., Stoel, M., Heikenwalder, M., Cahenzli, J., Velykoredko, Y., Balmer, M. L., Endt, K., Geuking, M. B., Curtiss, R. III, Mccoy, K. D., and Macpherson, A. J. (2010). Reversible microbial colonization of germ-free mice reveals the dynamics of IgA immune responses. *Science* 328, 1705–1709.

Hill, D. A., and Artis, D. (2010). Intestinal bacteria and the regulation of immune cell homeostasis. *Annu. Rev. Immunol.* 28, 623–667.

Ivanov, I. I., Atarashi, K., Manel, N., Brodie, E. L., Shima, T., Karaoz, U., Wei, D., Goldfarb, K. C., Santee, C. A., Lynch, S. V., Tanoue, T., Imaoka, A., Itoh, K., Takeda, K., Umesaki, Y., Honda, K., and Littman, D. R. (2009). Induction of intestinal Th17 cells by segmented filamentous bacteria. *Cell* 139, 485–498.

Iwata, M., Hirakiyama, A., Eshima, Y., Kagechika, H., Kato, C., and Song, S. Y. (2004). Retinoic acid imprints gut-homing specificity on T cells. *Immunity* 21, 527–538.

Kunisawa, J., Kurashima, Y., and Kiyono, H. (2011). Gut-associated lymphoid tissues for the development of oral vaccines. *Adv. Drug Deliv. Rev.* [Epub ahead of print].

Kunisawa, J., Mcghee, J., and Kiyono, H. (2007). "Mucosal S-IgA enhancement: development of safe and effective mucosal adjuvants and mucosal antigen delivery vehicles," in *Mucosal Immune Defense: Immunoglobulin A*, ed. C. Kaetzel (New York: Kluwer Academic/Plenum Publishers), 346–389.

Kunisawa, J., Nochi, T., and Kiyono, H. (2008). Immunological commonalities and distinctions between airway and digestive immunity. *Trends Immunol.* 29, 505–513.

Kunisawa, J., Takahashi, I., Okudaira, A., Hiroi, T., Katayama, K., Ariyama, T., Tsutsumi, Y., Nakagawa, S., Kiyono, H., and Mayumi, T. (2002). Lack of antigen-specific immune responses in anti-IL-7 receptor α chain antibody-treated Peyer's patch-null mice following intestinal immunization with microencapsulated antigen. *Eur. J. Immunol.* 32, 2347–2355.

Mantis, N. J., Cheung, M. C., Chintalacharuvu, K. R., Rey, J., Corthesy, B., and Neutra, M. R. (2002). Selective adherence of IgA to murine Peyer's patch M cells: evidence for a novel IgA receptor. *J. Immunol.* 169, 1844–1851.

Martinoli, C., Chiavelli, A., and Rescigno, M. (2007). Entry route of *Salmonella typhimurium* directs the type of induced immune response. *Immunity* 27, 975–984.

Mestecky, J., Moro, I., Kerr, M. A., and Woof, J. M. (2005). "Mucosal immunoglobulins," in *Mucosal Immunology*, 3rd Edn, eds J. Mestecky, M. E. Lamm, W. Strober, J. Bienenstock, J. R. Mcghee, and L. Mayer (San Diego: Academic Press), 153–182.

Michalek, S. M., Morisaki, I., Gregory, R. L., Kiyono, H., Hamada, S., and Mcghee, J. R. (1983). Oral adjuvants enhance IgA responses to *Streptococcus mutans*. *Mol. Immunol.* 20, 1009–1018.

Mora, J. R., Iwata, M., Eksteen, B., Song, S. Y., Junt, T., Senman, B., Otipoby, K. L., Yokota, A., Takeuchi, H., Ricciardi-Castagnoli, P., Rajewsky, K., Adams, D. H., and Von Andrian, U. H. (2006). Generation of gut-homing IgA-secreting B cells by intestinal dendritic cells. *Science* 314, 1157–1160.

Neutra, M. R., Mantis, N. J., and Kraehenbuhl, J. P. (2001). Collaboration of epithelial cells with organized mucosal lymphoid tissues. *Nat. Immunol.* 2, 1004–1009.

Nishikawa, S., Honda, K., Vieira, P., and Yoshida, H. (2003). Organogenesis of peripheral lymphoid organs. *Immunol. Rev.* 195, 72–80.

Obata, T., Goto, Y., Kunisawa, J., Sato, S., Sakamoto, M., Setoyama, H., Matsuki, T., Nonaka, K., Shibata, N., Gohda, M., Kagiyama, Y., Nochi, T., Yuki, Y., Fukuyama, Y., Mukai, A., Shinzaki, S., Fujihashi, K., Sasakawa, C., Iijima, H., Goto, M., Umesaki, Y., Benno, Y., and Kiyono, H. (2010). Indigenous opportunistic bacteria inhabit mammalian gut-associated lymphoid tissues and share a mucosal antibody-mediated symbiosis. *Proc. Natl. Acad. Sci. U.S.A.* 107, 7419–7424.

Rescigno, M. (2010). Intestinal dendritic cells. *Adv. Immunol.* 107, 109–138.

Spencer, J., Barone, F., and Dunn-Walters, D. (2009). Generation of immunoglobulin diversity in human gut-associated lymphoid tissue. *Semin. Immunol.* 21, 139–146.

Suzuki, K., Maruya, M., Kawamoto, S., Sitnik, K., Kitamura, H., Agace, W. W., and Fagarasan, S. (2010). The sensing of environmental stimuli by follicular dendritic cells promotes immunoglobulin A generation in the gut. *Immunity* 33, 71–83.

Suzuki, K., Meek, B., Doi, Y., Muramatsu, M., Chiba, T., Honjo, T., and Fagarasan, S. (2004). Aberrant expansion of segmented filamentous bacteria in IgA-deficient gut. *Proc. Natl. Acad. Sci. U.S.A.* 101, 1981–1986.

Talham, G. L., Jiang, H. Q., Bos, N. A., and Cebra, J. J. (1999). Segmented filamentous bacteria are potent stimuli of a physiologically normal state of the murine gut mucosal immune system. *Infect. Immun.* 67, 1992–2000.

Tezuka, H., Abe, Y., Iwata, M., Takeuchi, H., Ishikawa, H., Matsushita, M., Shiohara, T., Akira, S., and Ohteki, T. (2007). Regulation of IgA production by naturally occurring TNF/iNOS-producing dendritic cells. *Nature* 448, 929–933.

Tsuji, M., Komatsu, N., Kawamoto, S., Suzuki, K., Kanagawa, O., Honjo, T., Hori, S., and Fagarasan, S. (2009). Preferential generation of follicular B helper T cells from Foxp3+ T cells in gut Peyer's patches. *Science* 323, 1488–1492.

Weinstein, P. D., and Cebra, J. J. (1991). The preference for switching to IgA expression by Peyer's patch germinal center B cells is likely due to the intrinsic influence of their microenvironment. *J. Immunol.* 147, 4126–4135.

Yamamoto, M., Rennert, P., Mcghee, J. R., Kweon, M. N., Yamamoto, S., Dohi, T., Otake, S., Bluethmann, H., Fujihashi, K., and Kiyono, H. (2000). Alternate mucosal immune system: organized Peyer's patches are not required for IgA responses in the gastrointestinal tract. *J. Immunol.* 164, 5184–5191.

Yoshida, H., Honda, K., Shinkura, R., Adachi, S., Nishikawa, S., Maki, K., Ikuta, K., and Nishikawa, S. I. (1999). IL-7 receptor α^+ CD3- cells in the embryonic intestine induces the organizing center of Peyer's patches. *Int. Immunol.* 11, 643–655.

Conflict of Interest Statement: The authors declare that the research was conducted in the absence of any commercial or financial relationships that could be construed as a potential conflict of interest.

Received: 27 January 2012; paper pending published: 15 February 2012; accepted: 15 March 2012; published online: 02 April 2012.

Citation: Kunisawa J and Kiyono H (2012) Alcaligenes is commensal bacteria habituating in the gut-associated lymphoid tissue for the regulation of intestinal IgA responses. Front. Immun. 3:65. doi: 10.3389/fimmu.2012.00065

This article was submitted to Frontiers in Mucosal Immunity, a specialty of Frontiers in Immunology.

Membrane-bound human SCF/KL promotes in vivo human hematopoietic engraftment and myeloid differentiation

Shinsuke Takagi,[1-3] Yoriko Saito,[1] Atsushi Hijikata,[4] Satoshi Tanaka,[1,5,6] Takashi Watanabe,[4] Takanori Hasegawa,[7] Shinobu Mochizuki,[7] Jun Kunisawa,[5] Hiroshi Kiyono,[5] Haruhiko Koseki,[7] Osamu Ohara,[4,8] Takashi Saito,[3,9] Shuichi Taniguchi,[2] Leonard D. Shultz,[10] and Fumihiko Ishikawa[1]

[1]Research Unit for Human Disease Models, RIKEN Research Center for Allergy and Immunology, Yokohama, Japan; [2]Department of Hematology, Toranomon Hospital, Tokyo, Japan; [3]Department of Immune Regulation Research, Chiba University of Medical and Pharmaceutical Sciences, Chiba, Japan; [4]Laboratory for Immunogenomics, RIKEN Research Center for Allergy and Immunology, Yokohama, Japan; [5]Division of Mucosal Immunology, Institute of Medical Science, University of Tokyo, Tokyo, Japan; [6]Nippon Becton Dickinson Company, Tokyo, Japan; [7]Laboratory for Developmental Genetics, RIKEN Research Center for Allergy and Immunology, Yokohama, Japan; [8]Department of Human Gene Research, Kazusa DNA Research Institute, Kisarazu, Japan; [9]Laboratory for Cell Signaling, RIKEN Research Center for Allergy and Immunology, Yokohama, Japan; and [10]The Jackson Laboratory, Bar Harbor, ME

In recent years, advances in the humanized mouse system have led to significantly increased levels of human hematopoietic stem cell (HSC) engraftment. The remaining limitations in human HSC engraftment and function include lymphoid-skewed differentiation and inefficient myeloid development in the recipients. Limited human HSC function may partially be attributed to the inability of the host mouse microenvironment to provide sufficient support to human hematopoiesis. To address this problem, we created membrane-bound human stem cell factor (SCF)/KIT ligand (KL)–expressing NOD/SCID/IL2rgKO (hSCF Tg NSG) mice. hSCF Tg NSG recipients of human HSCs showed higher levels of both human CD45$^+$ cell engraftment and human CD45$^+$CD33$^+$ myeloid development compared with NSG recipients. Expression of hSCF/hKL accelerated the differentiation of the human granulocyte lineage cells in the recipient bone marrow. Human mast cells were identified in bone marrow, spleen, and gastrointestinal tissues of the hSCF Tg NSG recipients. This novel in vivo humanized mouse model demonstrates the essential role of membrane-bound hSCF in human myeloid development. Moreover, the hSCF Tg NSG humanized recipients may facilitate investigation of in vivo differentiation, migration, function, and pathology of human mast cells. (*Blood*. 2012;119(12): 2768-2777)

Introduction

The humanized mouse system, a xenogeneic transplantation and engraftment model for human hematopoietic stem cells (HSCs) and peripheral blood (PB) mononuclear cells (MNCs), facilitates the investigation of human hematopoietic and immune systems in vivo.[1,2] Since the pioneering work using SCID-hu[3] and Hu-PBL-SCID models,[4] investigators have attempted to better recapitulate human biology in mice across xenogeneic immunologic barriers. Recently, the introduction of targeted null mutations of immune-related genes, such as *Rag1, Rag2, Il2rg*, or *Prf1* in recipient mice, has improved engraftment levels of human CD45$^+$ leukocytes.[2,5-9] However, limitations remain in the ability of the host mouse hematopoietic microenvironment to support human hematopoiesis. The impaired development of human T-lymphoid and myeloid lineage cells compared with human B-lymphoid lineage cells in NOD/SCID and other immune-compromised mice may be the result of the lack of appropriate microenvironmental support. The recently created human leukocyte antigen (HLA) class I expressing immune-compromised NOD/SCID/IL2r γ null (NSG) mice partially addresses this issue for human T-cell development. Human CD8$^+$ T cells developing within these recipients of transplanted human HSCs exhibited cytokine production and cytotoxicity in an HLA-restricted manner.[10-12]

To create a hematopoietic microenvironment more suitable for human myeloid development, we developed a new immune-compromised mouse strain that expresses human membrane bound stem cell factor (SCF) under the control of the phosphoglycerate kinase (PGK) promoter (hSCF Tg NSG). Using hSCF Tg NSG mice as recipients of human HSCs, we aimed to clarify the role of membrane-bound form of SCF in supporting the engraftment of human hematopoietic cells and influencing the differentiation of the human myeloid lineage in the recipient mouse BM, spleen, and other organs. Here we show nearly complete human hematopoietic chimerism in the BM of hSCF Tg NSG recipients. In the BM of these recipients, human granulocytes accounted for the majority of engrafted human cells reflecting the physiologic human BM status. In addition to the development of immature and mature granulocytes, c-Kit$^+$ human mast cells differentiated efficiently in BM, spleen, and mucosal tissues. The hSCF Tg NSG mice, by supporting efficient human myeloid development including mast cells, may serve as a novel platform for in vivo investigation of human mast cell development and allergic responses.

Methods

Mice

NOD.Cg-*Prkdc*^{scid} *IL2rg*^{tm1Wjl} (NSG) mice and NOD.Cg-*Prkdc*^{scid} *IL2rg*^{tm1Wjl} Tg(PGK1-KITLG*220)441Daw/J, abbreviated as hSCF Tg NSG mice,

Submitted May 6, 2011; accepted October 2, 2011. Prepublished online as *Blood* First Edition paper, January 25, 2012; DOI 10.1182/blood-2011-05-353201.

The online version of this article contains a data supplement.

The publication costs of this article were defrayed in part by page charge payment. Therefore, and solely to indicate this fact, this article is hereby marked "advertisement" in accordance with 18 USC section 1734.

were generated at The Jackson Laboratory. The human membrane-bound SCF transgene driven by the human PGK promoter was backcrossed more than 10 generations from the original C3H/HeJ strain background[13] onto the NSG strain. All the mice were bred and maintained at The Jackson Laboratory and animal facility at RIKEN RCAI under defined flora according to guidelines established and approved by the Institutional Animal Committees at each respective institution.

Purification and transplantation of human HSCs

All experiments were performed with authorization from the Institutional Review Board for Human Research at RIKEN RCAI. Cord blood (CB) samples were first processed for isolation of MNCs using LSM lymphocyte separation medium (MP Biomedicals). CB MNCs were then enriched for human $CD34^+$ cells using anti–human CD34 microbeads (Miltenyi Biotec) and sorted for 7-AAD^- lineage (hCD3/hCD4/hCD8/hCD19/hCD56)$^-CD34^+CD38^-$ HSCs using FACSAria (BD Biosciences). To achieve high purity of donor HSCs, doublets were excluded by analysis of forward scatter (FSC)–height/FSC-width and side scatter (SSC)-height/SSC-width. Purity of each sorted sample was higher than 95%. Newborn (within 2 days of birth) hSCF Tg and non-Tg NSG recipients received 150 cGy total body irradiation using a ^{137}Cs-source irradiator, followed by intravenous injection of 5×10^2 to 5.3×10^4 sorted HSCs via the facial vein.

Analysis of human cell engraftment by flow cytometry

The recipient PB harvested from the retro-orbital plexus was evaluated for human hematopoietic engraftment every 3 to 4 weeks starting at 4 to 6 weeks after transplantation. After lysis of erythrocytes, cells were stained with anti-hCD45, anti-msCD45, anti-hCD3, anti-hCD19, anti-hCD33, and anti-hCD56 to determine human hematopoietic chimerism and to analyze cell lineages engrafted in the recipients. At 8 to 35 weeks after transplantation, the recipients were killed and single-cell suspensions of BM and spleen were analyzed using flow cytometry. Antibodies used for flow cytometry are specified in supplemental Methods (available on the *Blood* Web site; see the Supplemental Materials link at the top of the online article). The labeled cells were analyzed using FACSCantoII or FACSAria (BD Biosciences).

Morphologic analysis of cytospin specimens

Cytospin specimens of FACS-purified human myeloid cells were prepared with a Shandon Cytospin 4 cytocentrifuge (Thermo Electric) using standard procedures. To identify nuclear and cytoplasmic characteristics of each myeloid cell, cytospin specimens were stained with 100% May-Grünwald solution (Merck) for 3 minutes, followed by 50% May-Grünwald solution in phosphate buffer (Merck) for additional 5 minutes, and then with 5% Giemsa solution (Merck) in phosphate buffer for 15 minutes. All staining procedures were performed at room temperature. Light microscopy was performed with Zeiss Axiovert 200 (Carl Zeiss).

Microarray analysis

Purified $hCD45^+CD33^+$c-$Kit^-CD203c^-HLA\text{-}DR^-$ granulocytes and $hCD45^+CD33^+$ c-$Kit^-CD203c^-HLA\text{-}DR^+CD14^+$ monocytes from BM of 4 hSCF Tg NSG recipients and 3 non-Tg NSG recipients as well as neutrophils and monocytes from 2 healthy persons were evaluated using Human Genome U133 plus Version 2.0 GeneChips (Affymetrix). Total RNA was extracted with TRIzol (Invitrogen) from more than 10^4 sorted cells and amplified to cDNA using the Ovation Pico WTA System (Nugen). Biotinylated cDNA was synthesized with Two-Cycle Target Labeling Kit (Affymetrix). Microarray data were analyzed using the Bioconductor package (Bioconductor; http://www.bioconductor.org). The signal intensities of the probe sets were normalized using the GC-RMA program (Bioconductor). The RankProd program was used to select differentially expressed genes with a cutoff P value of less than .01 and an estimated false-positive rate of less than 0.05.[14] Gene annotation was obtained from Ingenuity Pathway Analysis and Gene Ontology Annotation databases (Ingenuity systems, http://www.ingenuity.com; Gene Ontology Annotation, http://www.ebi.ac.up/GOA). For differentially transcribed genes, GO term enrichment analysis was performed according to a method described by Draghici et al[15] with a correction of multiple testing using false discovery rate.[16] Eventually, GO terms with the false discovery rate-corrected P value $< .05$ were selected as functionally enriched terms. Raw data for microarray data are accessible at the RefDIC database (http://refdic.rcai.riken.jp) under the following accession numbers: RSM06616, RSM06617, RSM06618, RSM06620, RSM06621, RSM06622, RSM06623, RSM06633, RSM06642, RSM06648, RSM06665, RSM06667, RSM06668, RSM06669, RSM06670, RSM08241, and RSM08243. Differences in expression levels were considered significant if P is $< .05$ using Kruskal-Wallis, Wilcoxon-Mann-Whitney, or Student t test in KaleidaGraph (Synergy Software).

IHC and immunofluorescence imaging

Thin (~ 5-μm) sections prepared from paraformaldehyde-fixed paraffin-embedded tissues were stained with H&E using standard procedures. Immunohistochemistry (IHC) and immunofluorescence labeling were performed using standard procedures. Antibodies used for IHC and immunofluorescence labeling were mouse anti–human mast cell tryptase monocolonal antibody (Dako North America, clone AA1), mouse anti–human CD45 monoclonal antibody (Dako North America, clone $2B11^+PD7/26$), rabbit anti–human CD117 monoclonal antibody (Epitomics, clone YR145), and rabbit anti–human CD14 polyclonal antibody (Atlas Antibodies). Light microscopy was performed using an Axiovert 200 (Carl Zeiss). For quantification of $tryptase^+$ cell frequency, 3 high-power fields from 3 different recipients were examined using AutoMeasure module of AxioVision software (Release 4, Carl Zeiss). Confocal microscopy was performed using a LSM710 equipped with C-APOCHROMAT 40×/1.2 (Carl Zeiss).

Results

Human hematopoietic repopulation is enhanced in hSCF Tg NSG recipients

The humanized mouse model system has served as a tool to investigate human hematopoiesis, immunity, and diseases in vivo. However, one of the major limitations in the system is that the microenvironment supporting human hematopoiesis and immunity is primarily of mouse origin. In the present study, we created a strain of NSG mice expressing membrane-bound human SCF to analyze the role of the BM microenvironment in human hematopoietic lineage determination and development.

c-Kit, the receptor for SCF, is expressed at lower levels in human CB $Lin^-CD34^+CD38^-$ early HSCs and at high levels in mast cells.[17-19] For reconstitution of human myeloid and lymphoid cells, 5×10^2 to 5.3×10^4 FACS-purified CB $Lin^-CD34^+CD38^-$ HSCs were transplanted into newborn sublethally irradiated (1.5 Gy) hSCF Tg NSG mice and into non-Tg NSG controls (Table 1). To determine the kinetics of human hematopoietic chimerism in the recipient circulation, we performed flow cytometric analysis of PB every 3 to 4 weeks starting at 4 to 6 weeks after transplantation. During long-term observation, all the 21 hSCF Tg NSG recipient mice became moribund at 8 to 35 weeks after transplantation. Complete blood count analysis demonstrated reduced erythrocyte hemoglobin concentration in the PB of hSCF Tg NSG recipients compared with non-Tg NSG recipients (Figure 1A). Anemia in hSCF Tg NSG recipients was not associated with abnormalities in mean corpuscular volume, mean corpuscular hemoglobin, or mean corpuscular hemoglobin concentration (supplemental Figure 1). The suppression of host erythropoiesis in the hSCF Tg NSG recipients was related to the irradiation and engraftment of the human HSCs because unmanipulated nontransplanted hSCF Tg NSG mice did not develop anemia (supplemental Figure 1).

Table 1. Summary of hSCF Tg NSG and non-Tg NSG recipients analyzed

Recipient ID	CB ID	Graft dose	Survival, wks	CBC at time of death					% chimerism at time of death			% of CD45+ in BM				% of CD33+ in BM			% of CD45+ in BM			% chimerism of erythroid cells in BM
				WBC, $\times 10^3$/L	RBC, $\times 10^4/\mu$L	Hemoglobin, g/dL	Hematocrit, %	Platelets, $\times 10^3/\mu$L	PB	BM	Spleen	CD33+	CD3+	CD19+	CD3−CD56+	CD117+ CD203c+	HLA DR−	HLA DR+	CD117+ CD203c+	HLA DR−	HLA DR+	
N1-1	1	5000	21	1.1	500	10.0	35.0	550	75.5	93.3	95.3	31.1	1.2	50.2	0.3	0.9	51.5	47.6	0.3	16.0	14.8	NA
N1-2	1	5000	16	1.4	730	13.0	44.0	1100	42.6	76.1	72.9	35.2	0.1	54.8	0.4	0.7	39.6	59.7	0.2	13.9	21.0	NA
N1-3	1	5000	24	NA	NA	NA	NA	NA	20.7	12.6	4.4	32.9	3.8	60.7	0.0	4.4	37.9	57.7	1.0	12.5	19.0	3.1
S1-1	1	5000	23	4.1	220	6.7	15.6	150	99.1	99.7	94.4	77.2	24.5	19.2	0.5	3.9	80.6	15.5	3.0	62.2	11.9	NA
S1-2	1	5000	20	6.8	220	5.0	18.0	30	83.2	99.4	97.7	75.5	2.6	28.4	0.3	6.7	68.7	24.6	5.1	51.8	18.6	36.3
S1-3	1	5000	21	0.7	320	7.0	25.0	330	76.9	99.7	95.8	70.9	1.5	16.6	0.2	14.6	50.0	35.4	10.4	35.5	25.1	0.0
S1-4	1	500	26	0.5	150	3.0	11.0	250	30.7	97.0	86.3	69.0	2.0	47.5	0.1	6.9	68.6	24.5	4.8	47.3	16.9	NA
N2-1	2	10 000	35	0.8	390	8.0	30.0	110	31.7	54.9	87.1	50.3	21.8	25.8	2.4	19.1	7.4	73.5	9.6	3.7	37.0	11.5
S2-1	2	10 000	16	1.3	186	4.1	13.2	583	90.7	96.6	99.3	18.7	3.2	40.6	1.2	34.4	18.0	47.6	6.4	3.4	8.9	NA
S3-1	3	10 000	13	0.2	215	3.9	12.6	793	52.0	97.8	90.9	54.2	0.0	42.8	0.7	19.0	44.6	36.4	10.3	24.2	19.7	NA
S3-2	3	10 000	15	2.2	161	3.1	9.8	458	93.6	99.6	98.2	61.5	4.4	20.4	1.4	7.3	60.5	32.2	4.5	37.2	19.8	NA
S4-1	4	10 000	13	0.5	97	1.9	5.1	6	98.6	100.0	98.2	52.0	1.2	39.8	0.3	2.7	81.9	15.4	1.4	42.6	8.0	27.2
N5-1	5	12 000	35	3.1	310	7.0	25.0	550	6.8	36.8	48.9	29.9	17.5	41.9	NA	22.6	7.0	70.4	6.8	2.1	21.1	5.8
N6-1	6	14 000	23	2.1	520	10.0	34.0	620	57.6	65.0	83.6	29.3	17.6	43.1	1.6	3.3	45.1	51.6	1.0	13.2	15.1	7.4
N6-2	6	14 000	21	1.6	680	12.0	40.0	660	64.6	25.3	81.5	10.4	17.2	64.4	0.5	33.9	17.5	48.6	3.5	1.8	5.1	1.4
N6-3	6	14 000	24	2.3	490	10.0	33.0	80	73.8	71.8	92.8	18.5	13.9	51.1	0.8	10.6	8.5	81.4	2.0	1.6	15.1	12.8
S6-1	6	14 000	16	2.2	236	4.5	15.5	33	70.0	88.5	94.7	39.4	5.8	43.6	0.7	68.9	8.1	23.0	27.1	3.2	9.1	33.1
S6-2	6	14 000	14	4.6	270	6.0	21.0	108	85.4	90.0	95.2	33.3	11.6	46.8	0.9	36.5	16.0	47.5	12.2	5.3	15.8	5.8
S7-1	7	15 000	16	4.9	293	6.1	19.4	132	93.6	99.7	98.8	76.5	1.4	42.3	0.6	1.6	80.1	18.3	1.2	61.3	14.0	NA
S8-1	8	16 000	13	1.0	183	3.3	9.4	78	98.6	100.0	99.7	16.2	19.9	52.1	0.9	25.1	1.0	73.9	4.1	0.2	12.0	NA
S8-2	8	16 000	11	1.0	376	5.6	18.4	568	89.5	99.6	98.5	48.6	0.2	54.5	0.6	4.9	42.0	53.1	2.4	20.4	25.8	NA
N9-1	9	18 000	20	2.7	650	13.0	42.0	130	71.6	87.2	92.0	15.0	1.7	72.4	0.4	1.4	24.7	74.0	0.2	3.7	11.1	9.8
S9-1	9	18 000	16	1.4	164	3.4	10.6	80	90.4	99.9	97.0	51.4	0.2	35.1	0.2	2.4	54.9	42.7	1.2	28.2	21.9	25.5
N10-1	10	20 000	19	1.0	660	12.0	42.0	77	38.4	46.5	87.1	25.9	44.4	24.1	0.8	3.9	6.2	89.9	1.0	1.6	23.3	12.0
N10-2	10	20 000	14	NA	NA	NA	NA	NA	NA	NA	NA	NA	NA	NA	NA	NA	NA	NA	NA	NA	NA	NA
N10-3	10	20 000	12	NA	NA	NA	NA	NA	NA	NA	NA	NA	NA	NA	NA	NA	NA	NA	NA	NA	NA	NA
S10-1	10	20 000	19	2.5	292	6.1	20.9	6	95.5	99.7	97.3	42.3	14.4	35.5	0.9	5.7	28.8	65.5	2.4	12.2	27.7	4.3
S10-2	10	20 000	14	1.5	170	3.0	11.0	30	95.8	99.7	89.3	27.3	28.4	28.0	5.4	18.6	19.8	61.6	5.1	5.4	16.8	17.1
N11-1	11	36 000	20	25.1	470	9.0	31.0	240	84.1	70.7	94.0	19.5	5.9	63.6	0.7	3.8	17.8	78.4	0.7	3.5	15.3	42.3
S11-1	11	36 000	10	19.2	420	8.0	27.0	410	77.5	98.0	95.3	34.0	0.2	43.5	0.5	4.5	34.6	60.9	1.5	11.8	20.7	58.5
N12-1	12	53 000	8	NA	NA	NA	NA	NA	36.9	95.6	83.3	20.3	0.0	72.2	0.2	NA	NA	NA	NA	NA	NA	NA
S12-1	12	53 000	11	NA	NA	NA	NA	NA	100.0	100.0	99.9	43.5	6.5	39.1	1.5	NA	NA	NA	NA	NA	NA	NA
S12-2	12	53 000	8	NA	NA	NA	NA	NA	93.1	100.0	NA	65.6	0.2	13.2	NA	1.6	83.7	14.7	1.0	54.9	9.6	NA
S12-3	12	53 000	13	13.6	211	3.9	10.9	165	57.0	79.5	68.3	47.5	12.5	35.7	2.2	8.8	59.9	31.3	4.2	28.5	14.9	NA
N13-1	13	17 000	20	6.4	720	13.0	45.0	470	39.2	85.0	81.8	21.8	0.0	69.0	0.2	0.4	46.1	53.5	0.1	10.0	11.7	7.6
S13-1	13	17 000	20	2.8	290	7.0	27.0	510	74.9	93.7	94.5	38.1	6.0	47.8	0.4	26.6	31.3	42.1	10.1	11.9	16.0	48.4

A total of 21 human HSC-engrafted hSCFTg NSG (S) recipients and 15 human HSC-engrafted non-Tg NSG (N) recipients were created.
WBC indicates white blood cell count; RBC, red blood cell count; and NA, not applicable.

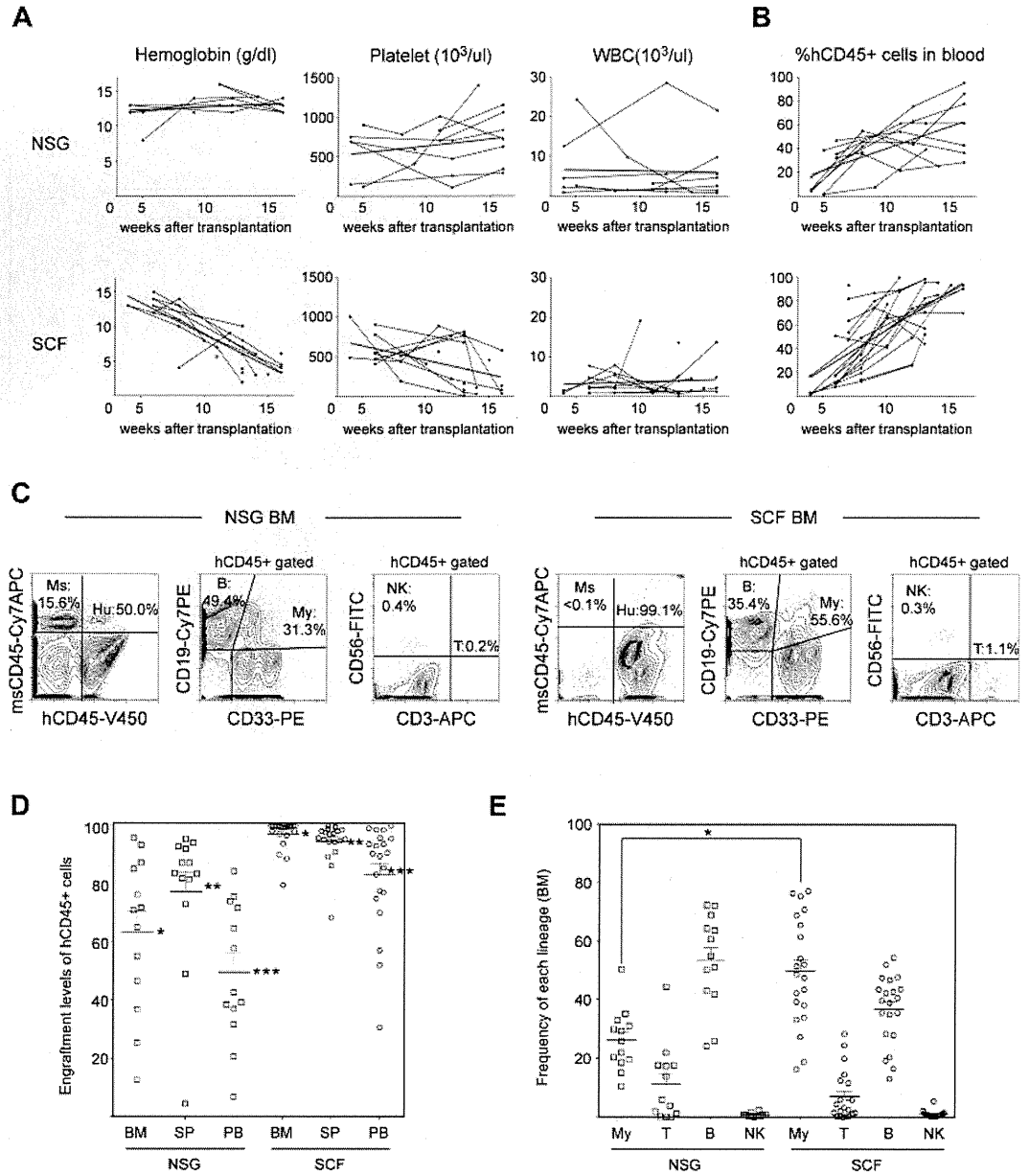

Figure 1. Human hematopoietic engraftment is enhanced in hSCF Tg NSG recipients. (A) hSCF Tg NSG recipients developed progressive anemia as evidenced by reduced hemoglobin concentration compared with non-Tg NSG mice transplanted with human HSCs from the same donor source. (B) Human CD45$^+$ chimerism was analyzed over time in PB of hSCF Tg and non-Tg NSG recipients. (C) Representative flow cytometric contour plots demonstrating the presence of human CD45$^+$ cells, CD19$^+$ B cells, CD33$^+$ myeloid cells, CD3$^+$ T cells, and CD56$^+$CD3$^-$ NK cells in recipient BM. (D) At the time of death, engraftment levels of human CD45$^+$ cells in the BM, spleen, and PB of hSCF Tg NSG recipients were significantly higher compared with non-Tg NSG controls (BM: hSCF Tg n = 21, non-Tg n = 13, $P < .0001$; spleen: hSCF Tg n = 21, non-Tg n = 13, $P = .0065$; PB: hSCF Tg n = 21, non-Tg n = 13, $P < .0001$). (E) In hSCF Tg NSG recipient BM, significantly greater human CD33$^+$ myeloid lineage development was observed (hSCF Tg n = 21, non-Tg n = 13, $P = .0002$).

Impaired mouse erythropoiesis in these engrafted hSCF Tg NSG mice was associated with rapid expansion of hCD45$^+$ hematopoietic cells compared with non-Tg NSG recipients (Figure 1B).

At 8 to 35 weeks after transplantation, individual hSCF Tg NSG recipients were analyzed to determine levels of reconstitution of human hematopoiesis and immunity in the BM, spleen, and PB. At the time of necropsy, we did not observe any gross macroscopic abnormalities in these recipients. We performed flow cytometric analysis to evaluate the engraftment levels of human CD45$^+$ cells (calculated as % hCD45$^+$ cells relative to total numbers of mouse and human CD45$^+$ cells in the nucleated cell gate). Engraftment levels of human CD45$^+$ leukocytes in the BM, spleen, and PB were significantly higher in hSCF Tg NSG recipients (mean ± SEM; 97.1% ± 1.1%, 94.5% ± 1.6%, and 83.1% ± 3.9%, respectively; n = 21) compared with engrafted non-Tg NSG recipients (63.1% ± 7.3%, 77.3% ± 6.9%, and 49.5% ± 6.5%, respectively; n = 13; $P < .0001$, $P = .0065$, and $P < .0001$ by 2-tailed t test, respectively; Figure 1C-D). Compared with enhanced engraftment of human leukocytes in the recipient BM, development of human erythroid precursors was not significantly different in hSCF Tg NSG recipients compared with non-Tg NSG recipients (hSCFTg: 25.6% ± 6.1%; n = 10 and non-Tg NSG controls: 11.4% ± 3.6%; n = 10; $P = .0601$; supplemental Figure 2). We next analyzed the development of human lymphoid and myeloid cells in the engrafted human CD45$^+$ hematopoietic cell populations by flow cytometry using monoclonal antibodies against hCD3, hCD19,

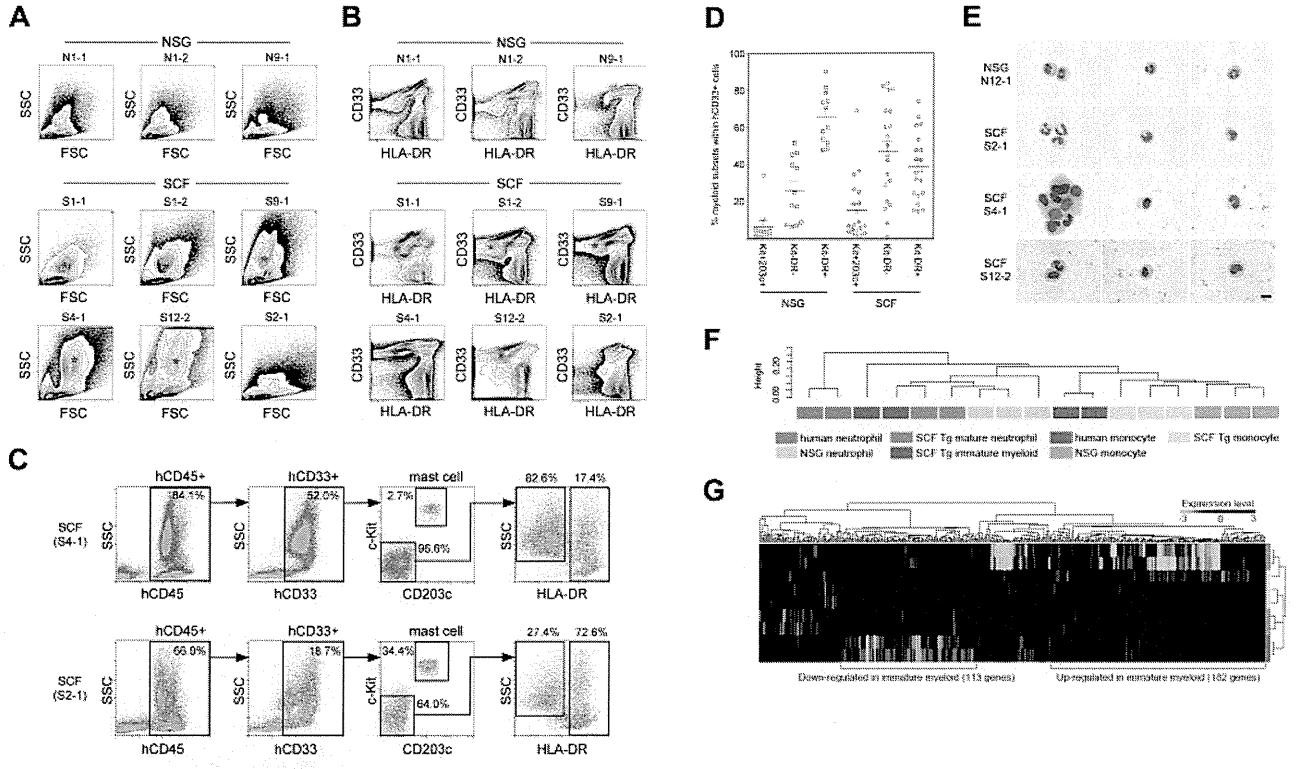

Figure 2. HLA-DR-negative human myeloid cells predominate in hSCF Tg NSG recipient BM. (A) Flow cytometric contour plots demonstrating FSC and SSC characteristics of 6 hSCF Tg NSG recipient BM (S1-1, S1-2, S9-1, S4-1, S12-2, and S2-1) and 3 non-Tg NSG recipient BM (N1-1, N1-2, and N9-1). Polymorphonuclear myeloid cells (red asterisks) are present at high frequencies in hSCF Tg NSG recipient BM. (B) Flow cytometry contour plots demonstrating hCD33 and HLA-DR expression in the same recipients as shown in panel A. Consistent with their FSC and SSC characteristics, hSCF Tg NSG recipient BM contained a prominent $CD33^+HLA\text{-}DR^-$ granulocyte population (red asterisks; N1-1, killed at 21 weeks; N1-2, killed at 16 weeks; N9-1, killed at 20 weeks; S1-1, killed at 23 weeks; S1-2, killed at 20 weeks; S9-1, killed at 16 weeks; S4-1, killed at 13 weeks; S12-2, killed at 8 weeks; and S2-1, killed at 16 weeks). (C) Representative flow cytometric scatter plots of hSCF Tg NSG recipient BM demonstrating the identification of human $c\text{-}Kit^+CD203c^+$ mast cells within the $hCD33^+$ fraction and $HLA\text{-}DR^-SSC^{high}$ granulocytes and $HLA\text{-}DR^+SSC^{low}$ APCs within the $c\text{-}Kit^-CD203c^-$ fraction (S4-1, killed at 13 weeks; and S2-1, killed at 16 weeks). (D) Frequencies of human $c\text{-}Kit^+CD203c^+$ mast cells, $CD33^+HLA\text{-}DR^-$ granulocytes, and $CD33^+HLA\text{-}DR^+$ APCs within the total $hCD45^+hCD33^+$ myeloid cell population in the BM of hSCF Tg and non-Tg NSG recipients. Numbers of cells in the granulocyte/neutrophil fraction were significantly higher in hSCF Tg NSG recipient BM (hSCF Tg n = 20, non-Tg n = 12, $P = .0001$). (E) $CD33^+HLA\text{-}DR^-$ cells from hSCF Tg and non-Tg NSG recipient BM were FACS-purified and examined by MGG staining. In 9 of 13 hSCF Tg recipients (S4-1 and S12-2 shown as representative), immature myeloid cells composed the majority of cells in this fraction. In 4 of 13 hSCF Tg recipients (S2-1 shown as representative) and 4 of 5 non-Tg NSG recipients (N12-1 shown as representative), mature neutrophils (band and segmented forms) were observed (N12-1, killed at 8 weeks; S2-1, killed at 16 weeks; S4-1, killed at 13 weeks; and S12-2, killed at 8 weeks). (F-G) Global transcriptional profiles of FACS-purified $CD33^+cKit^-CD203^-HLA\text{-}DR^-$ granulocytes and $CD33^+c\text{-}Kit^-CD203c^-HLA\text{-}DR^+CD14^+$ monocytes derived from hSCF Tg NSG and non-Tg NSG recipient BM as well as human $CD16^+$ neutrophils and $CD14^+$ monocytes were compared. (F) Unsupervised clustering for each group is shown. (G) The expression heatmap demonstrates genes that are significantly under- and over-represented in each population.

hCD56, and hCD33 along with anti–human and anti–mouse CD45 antibodies (Figure 1C,E). Although there was recipient-to-recipient variability, the frequency of human $CD33^+$ myeloid cells within the total human $CD45^+$ population was significantly higher in the hSCF Tg NSG recipient BM than in the non-Tg NSG recipient BM and constituted the majority of human hematopoietic cells (hSCF Tg: 49.7% ± 4.0%; n = 21 and non-Tg NSG controls: 26.2% ± 2.9%; n = 13; $P = .0002$ by 2-tailed t test). In contrast, in non-Tg NSG recipients, the majority of human hematopoietic cells in the BM were B cells (53.3% ± 4.5%; n = 13), consistent with previous reports.[5,9,20] These findings demonstrate that the expression of membrane-bound hSCF in BM microenvironment results in significantly more efficient engraftment of human HSCs as well as enhanced development of human $CD33^+$ myeloid cells from the engrafted human HSCs.

Human myeloid lineage development in hSCF Tg NSG recipients

Next, we examined the development of human myeloid subsets in the human membrane-bound SCF-expressing BM microenvironment. Flow cytometric scatter plots demonstrate the development of the SSC high granulocyte fraction in hSCF Tg NSG recipients, which correlate with $CD33^+HLA\text{-}DR^-$ cells (Figure 2A-B). To quantify the frequencies of different myeloid subsets in these recipients, we first identified $CD33^+c\text{-}Kit^+CD203c^+$ mature human mast cells among human $CD45^+$ cells. Next, we identified $CD33^+HLA\text{-}DR^-$ human granulocyte lineage cells and human $CD33^+HLA\text{-}DR^+$ antigen-presenting cells (APCs) among human $CD45^+$ cells excluding mature mast cells (Figure 2C).

In the hSCF Tg NSG recipient BM, there were increased percentages of $CD33^+HLA\text{-}DR^-$ granulocytes and decreased percentages of $CD33^+HLA\text{-}DR^+$ APCs compared with non-Tg NSG controls (hSCF Tg: 46.7% ± 5.9% and 38.3% ± 4.0%, respectively; n = 20 and non-Tg NSG controls: 25.8% ± 5.0% and 65.5% ± 4.1%, respectively; n = 12; $P = .0204$ and $P = .0001$ by 2-tailed t test, respectively; Figure 2D). In the BM of 11 of 20 hSCF Tg NSG recipients examined, $c\text{-}Kit^-CD203c^-HLA\text{-}DR^-$ SSC^{high} granulocytes accounted for the highest frequency of total human myeloid cells (Figure 2D; Table 1). To examine the morphologic features of the human granulocytes developing in the hSCF Tg recipients, we carried out May-Grünwald-Giemsa (MGG) staining using cytospin specimens of FACS-purified $CD33^+c$-

$Kit^-CD203c^-HLA\text{-}DR^-$ cells from BM of hSCF Tg and non-Tg NSG recipients. In 9 of 13 hSCF Tg recipient BM cells examined, the majority of myeloid cells showed the morphology of immature granulocytes with large nuclear-to-cytoplasmic ratio and nuclei with few lobulations, largely consisting of myelocytes and metamyelocytes (S4-1 and S12-2 shown as representative in Figure 2E). In 4 of 13 hSCF Tg recipients examined and in 4 of 5 non-Tg NSG recipients, mature segmented neutrophils were present in the sorted $CD33^+c\text{-}Kit^-CD203c^-HLA\text{-}DR^-$ granulocyte population (N12-1 and S2-1 shown as representative in Figure 2E). These findings indicate that both by quantitative and morphologic examinations, human granulocytic cells with various degrees of maturity predominate among the $CD33^+$ myeloid cells developing within the hSCF Tg NSG recipients. To examine the myeloid differentiation capacity of hematopoietic stem and progenitor populations in a functional manner, we performed a colony-forming cell assay using $CD34^+CD38^-$ and $CD34^+CD38^+$ cells derived from BM of hSCF Tg NSG recipients and non-Tg NSG recipients. In both cell populations, myeloid and erythroid colony formation were similar between hSCF Tg NSG and non-Tg NSG recipient BM (supplemental Figure 3).

We then analyzed global transcriptional profiles of $CD33^+HLA\text{-}DR^-c\text{-}Kit^-CD203c^-$ granulocytes from hSCF Tg NSG recipient BM (n = 4), non-Tg NSG recipient BM (n = 3), and primary human BM (n = 2). Additional control samples included BM monocytes from hSCF Tg recipients (n = 3), non-Tg NSG recipient BM monocytes (n = 3), and primary human BM monocytes (n = 2). Unsupervised clustering demonstrated a clear segregation of transcriptional profiles between granulocytes and monocytes regardless of the source. This suggests that human granulocytes and monocytes in humanized mouse undergo a distinct differentiation process similar to their counterparts in human BM (Figure 2F). We next examined whether there were any differences in gene expression within 3 distinct granulocyte sources (hSCF Tg recipient BM, non-Tg NSG recipient BM, and primary human BM neutrophils; Figure 2G). As seen in the heatmap representation, we found clusters of genes differentially transcribed in the distinct sources of granulocytes (Figure 2G). Multiple genes associated with transcriptional regulation were included in the genes upregulated in human immature granulocytes derived from the BM of hSCF Tg NSG mice, suggesting that these cells are more actively cycling and proliferating compared with mature granulocytes from the BM of hSCF Tg NSG and non-Tg NSG mice and primary human BM neutrophils (Figure 2G; supplemental Tables 1 and 2).

Development of human mast cells in hSCF Tg NSG recipients

We next investigated the development of human mast cells in the membrane-bound hSCF-expressing NSG mice. Overall, the frequencies of $cKit^+CD203c^+$ cells within total BM $CD33^+$ myeloid cells were similar between hSCF Tg NSG and non-Tg NSG recipients when excluding 2 non-Tg NSG recipients observed for more than 8 months ($P = .1439$ by 2-tailed t test; Figure 2D; Table 1). In 7 of 20 hSCF Tg NSG recipients, compared with one of 10 non-Tg NSG recipients, the frequency of $cKit^+CD203c^+$ cells in BM $CD33^+$ cells was greater than 15% (Figure 2D; Table 1). When these $cKit^+CD203c^+$ cells were FACS-purified and examined by MGG staining, their morphology was consistent with mast cells with various degrees of cytoplasmic granulation (Figure 3A-B). Histologic examination of H&E-stained bone sections showed increased cellularity in hSCF Tg NSG recipients compared with non-Tg NSG recipients (Figure 3C). We then performed IHC staining for mast cell tryptase to identify human mast cells in the BM. Consistent with the quantitative analysis by flow cytometry, $tryptase^+$ cells were abundantly observed in the hSCF Tg NSG recipients compared with non-Tg NSG recipients (Figure 3C). This does not reflect an increase in mouse mast cells because nearly all nucleated hematopoietic cells in the hSCF Tg NSG recipients are of human origin (Figure 1D). The same sections were further subjected to the immunofluorescence staining followed by confocal imaging demonstrating that these are mast cells and not $CD14^+$ monocytes (supplemental Figure 4).

Mast cell progenitors and mature mast cells reside in high frequencies in the spleen of normal immunocompetent mice.[21] We next examined the spleen of human HSC-engrafted hSCF Tg NSG recipients. Human $CD33^{high}c\text{-}Kit^+CD203c^+$ mast cells accounted for the highest frequency among total $hCD45^+hCD33^+$ myeloid cells in the spleen of both hSCF Tg NSG and non-Tg NSG HSC-engrafted recipients (Figure 4A-B). However, the frequencies of human mast cells in the myeloid cell population were significantly higher in hSCF Tg NSG recipients than in non-Tg NSG controls (hSCF Tg: 77.4% ± 4.5%; n = 20 and non-Tg NSG controls: 62.5% ± 3.9%; n = 12; $P = .0304$ by 2-tailed t test; Figure 4B). These human cells with surface expression phenotype of mast cells also showed morphologic features of mature mast cells (Figure 4C). Mast cell tryptase IHC staining confirmed the presence of human mast cells within the recipient spleen (Figure 4D). These findings indicate that the expression of membrane-bound human SCF in the recipient mouse microenvironment enhances development of human mast cells from transplanted human HSCs within hematopoietic organs, such as the BM and spleen, consistent with the activation of c-Kit signaling.

Next, we investigated whether the transgenic expression of hSCF results in the efficient development of mucosal tissue-type human mast cells in respiratory and gastrointestinal mucosal layers, as well as in hematopoietic organs. For this purpose, we performed IHC staining of human tryptase-expressing mast cells in the lung, stomach, small intestine, and large intestine in hSCF Tg NSG and non-Tg NSG recipients. In the hSCF Tg NSG recipient lungs, human tryptase-positive mast cells were identified within cellular infiltrates (supplemental Figure 5). In tissue sections from the stomach, small intestine, and large intestine, human tryptase-positive mast cells were present in both hSCF Tg NSG and non-Tg NSG recipients (Figure 5A-B). The mast cell $tryptase^+$ cells in gastrointestinal tissues of hSCF Tg mice were further examined by immunofluorescence microscopy using anti–human CD45 and anti–human-c-Kit antibodies. We found the presence of $hCD45^+c\text{-}Kit^+$ cells in the gastric tissues of the hSCF Tg recipients consistent with IHC staining for mast cell tryptase (Figure 5C). Because gastric tissue is one of the major sites of mast cell populations in humans and mice, we quantified human mast cells in the gastric tissue of hSCF Tg and non-Tg NSG recipients transplanted with human HSCs. IHC staining for human mast cell tryptase followed by quantification of $tryptase^+$ cells demonstrated the presence of human mast cells in gastric tissues of hSCF Tg NSG recipients (7.01% ± 0.63%, 3 sites per recipient analyzed in 3 mice) compared with non-Tg NSG recipients (2.53% ± 0.53%, 3 sites per recipient analyzed in 3 mice; $P < .0001$ by 2-tailed t test; Figure 5D). Collectively, transgenic expression of human membrane-bound SCF influences human myeloid development and mast cell development in hematopoietic organs and mucosal tissues along with the achievement of high chimerism of human hematopoietic cells in hematopoietic organs.

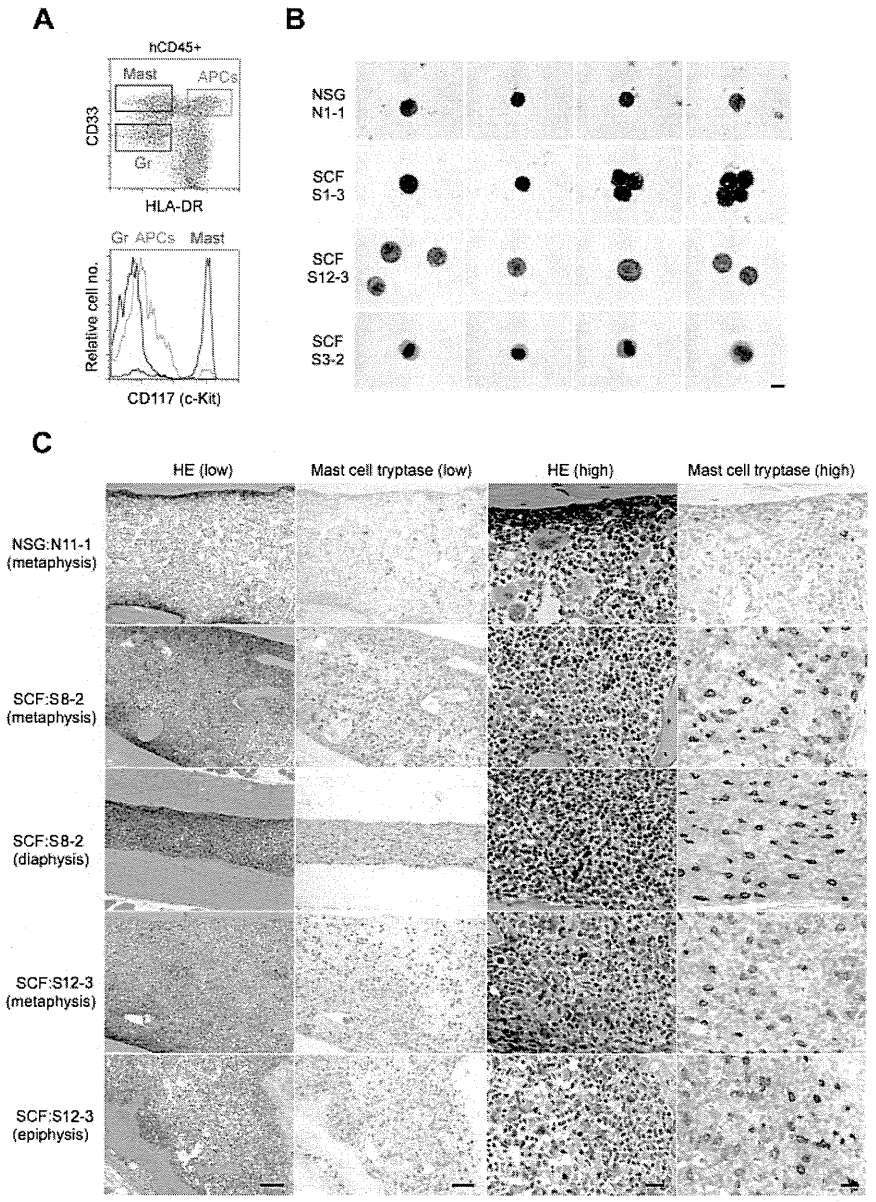

Figure 3. Human mast cell development in hSCF Tg NSG recipient BM. (A) Representative flow cytometric scatter plot and histogram demonstrating the identification of human $CD45^+CD33^+CD117^+$ mast cells. (B) FACS-sorted $hCD45^+CD33^+CD117^+CD203c^+$ human mast cells from a representative non-Tg NSG recipient BM (N1-1, 0.9% human mast cells within $hCD45^+CD33^+$ population) and hSCF Tg NSG recipient BM (S1-3, 14.6%; S12-3, 8.8%; and S3-2, 7.3% human mast cells within the $hCD45^+CD33^+$ population) were examined by MGG staining (N1-1, killed at 21 weeks; S1-3, killed at 21 weeks; S12-3, killed at 13 weeks; and S3-2, killed at 15 weeks). (C) H&E- and anti-mast cell tryptase antibody–stained bone sections demonstrate hypercellular BM with high frequency of $tryptase^+$ human mast cells in hSCF Tg NSG recipients. Non-Tg NSG recipient: N11-1, 70.7% $hCD45^+$. hSCF Tg NSG recipients: S8-2, 99.6%; and S12-3, 79.5% $hCD45^+$ (N11-1, killed at 20 weeks; S8-2, killed at 11 weeks; and S12-3, killed at 13 weeks).

Discussion

A supportive microenvironment is essential for hematopoietic and immune system homeostasis. Critical roles played by various niches in the maintenance of cell cycle quiescence and self-renewal capacity of HSCs have been demonstrated, and the thymic microenvironment is critical for T-cell education.[22,23] However, despite significant progress over the last decade, the stromal microenvironment within the humanized mouse is predominately of mouse origin. Although several key molecules, such as SDF1, are cross-reactive between human and mouse, a humanized microenvironment is required both to further improve human hematopoietic development in the recipients and to investigate in vivo the interactions between hematopoietic cells and their microenvironment.

In the present study, we humanized membrane-bound stem cell factor [SCF = KIT ligand (KL)] using the construct and mouse strain created by Majumdar et al.[13] Toksoz et al reported that human membrane-bound SCF expressed by mouse stromal cells efficiently supports long-term human hematopoiesis in vitro.[24] The importance of SCF interaction with $cKit^+$ HSCs and mast cell progenitors in murine hematopoiesis is highlighted by the hematopoietic abnormalities in mice with *Kitl* and *Kit* mutations.[25-27] In human hematopoiesis, SCF-cKit signaling is critical for the maintenance of stem and progenitor cell activities.[28] Human SCF/KL has been shown to drive cell-cycle entry by primitive hematopoietic cells in vitro.[29] Both long-term colony-initiation and colony-forming capacities are expanded ex vivo by cytokine supplementation that includes SCF/KL.[30-32] Therefore, to elucidate the role of membrane-bound human SCF in differentiation, proliferation, and maturation of human hematopoiesis in vivo, we created a novel NSG mouse strain that can support the engraftment of human HSCs and express hSCF in microenvironment. In hSCF Tg NSG recipients transplanted with human HSCs, the engraftment levels of human $CD45^+$ cells were significantly higher compared with non-Tg NSG controls. Majumdar et al reported that human SCF binds mouse c-Kit receptor but that the binding affinity is

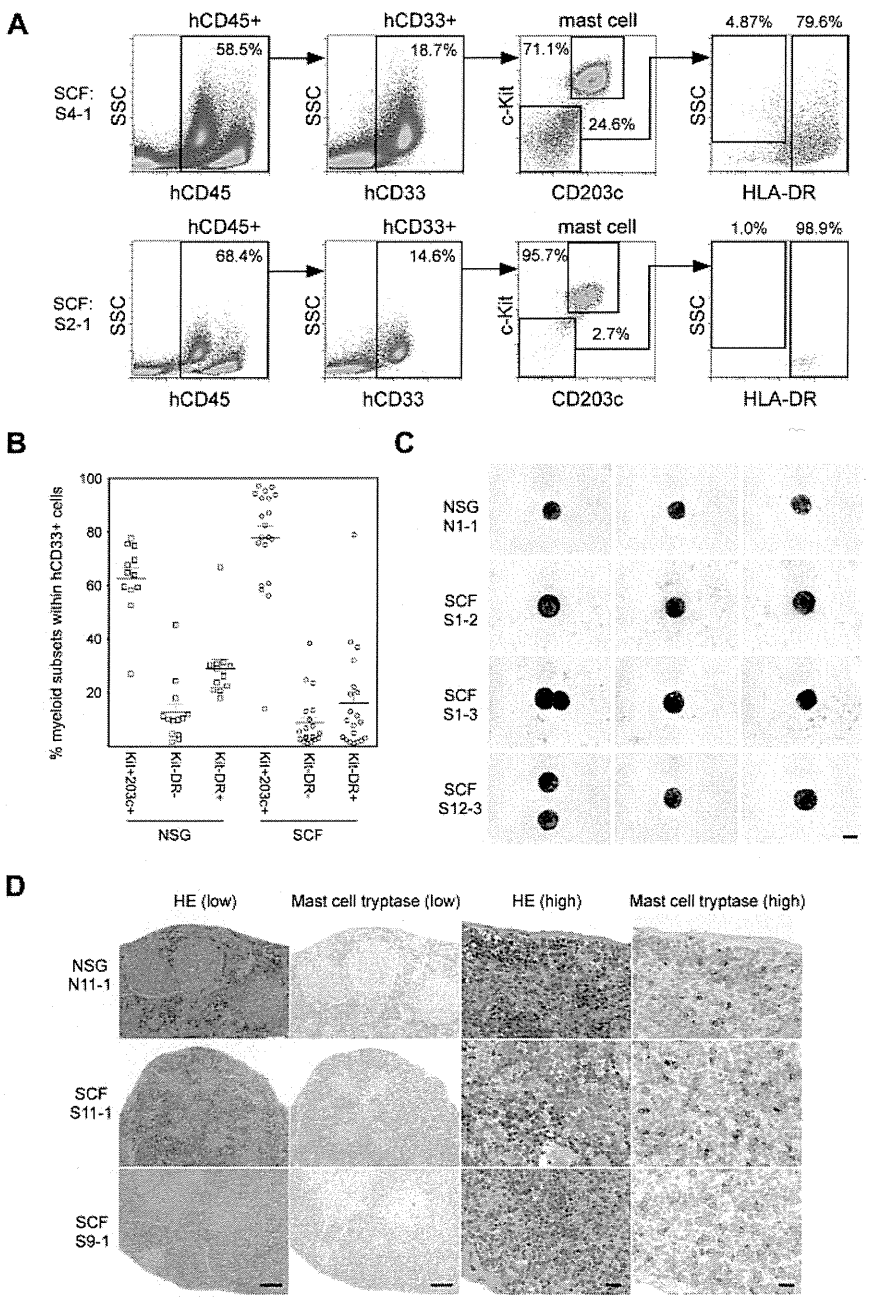

Figure 4. Human mast cell development in hSCF Tg NSG recipient spleen. (A) Human mast cell development is enhanced in hSCF Tg NSG recipient spleens (S4-1, killed at 13 weeks; and S2-1, killed at 16 weeks). (B) Frequencies of human c-Kit$^+$CD203c$^+$ mast cells, CD33$^+$HLA-DR$^-$ granulocyte population, and CD33$^+$HLA-DR$^+$ APCs within total hCD45$^+$hCD33$^+$ myeloid cells in the spleens of hSCF Tg and non-Tg NSG recipients. Human mast cell development in the spleen was significantly greater in the hSCF Tg NSG recipients (hSCF Tg: n = 20, non-Tg NSG: n = 12, $P = .0304$). (C) FACS-sorted hCD45$^+$CD33$^+$CD117$^+$CD203c$^+$ human mast cells from a representative non-Tg NSG recipient spleen (N1-1, 59.3% human mast cells within hCD45$^+$CD33$^+$ population) and hSCF Tg NSG recipient spleen (S1-2, 85.7%; S1-3, 77.7%; and S12-3, 56.1% human mast cells within hCD45$^+$CD33$^+$ population) were examined by MGG staining (N1-1, killed at 21 weeks; S1-2, killed at 20 weeks; S1-3, killed at 21 weeks; and S12-3, killed at 13 weeks). (D) H&E- and anti–mast cell tryptase antibody–stained spleen sections demonstrating the presence of human mast cells in non-Tg NSG recipients and hSCF Tg NSG recipients (non-Tg NSG recipient: N11-1, 94.0% hCD45$^+$; hSCF Tg NSG recipients: S11-1, 95.3%; and S9-1, 97.0% hCD45$^+$; N11-1, killed at 20 weeks; S11-1, killed at 10 weeks; and S9-1, killed at 16 weeks).

weaker compared with the binding affinity of human SCF to human c-Kit.[13] Therefore, the significant improvement of human hematopoietic chimerism could be attributed to preferential binding of human SCF to human HSCs instead of murine c-Kit$^+$ HSCs resulting in accelerated signaling through c-Kit in human HSCs and by impaired or attenuated support of mouse HSCs.[1,33,34] Presumably because of the competition between human and mouse hematopoietic stem or myeloid/erythroid progenitor cells, we observed diminished mouse erythrocyte hemoglobin concentration with normal range of mean corpuscular volume, mean corpuscular hemoglobin, and mean corpuscular hemoglobin concentration in all the 21 hSCF Tg NSG recipients but not in any of the non-Tg NSG recipients or nontransplanted hSCF Tg NSG adults. In addition to the greatly increased levels of human hematopoietic repopulation, we identified significant differences in human hematopoietic differentiation in hSCF Tg NSG recipients compared with non-Tg NSG recipients. Namely, there were substantially increased levels of human myeloid differentiation from HSCs in the hSCF Tg NSG mice, whereas human B cells accounted for the greatest population in the BM of non-Tg NSG mice. Because normal human BM contains myeloid cells at a relatively high frequency (36.2%-62.2%),[35] human SCF may be important in recapitulating human BM myelopoiesis in immunodeficient mice. In addition, membrane-bound human SCF may exert distinct effects on human myeloid development in the BM and in the spleen. In the BM of hSCF Tg recipients, the majority of human myeloid cells were c-Kit$^-$CD203c$^-$HLA-DR$^-$ granulocytes. Among these granulocytes, myeloid cells at various levels of maturity were identified, with myelocytes and metamyelocytes predominating in the majority of hSCF Tg NSG recipients. Because immature cells were more prominent in hSCF Tg NSG recipients compared with non-Tg NSG recipients, we performed microarray analysis to

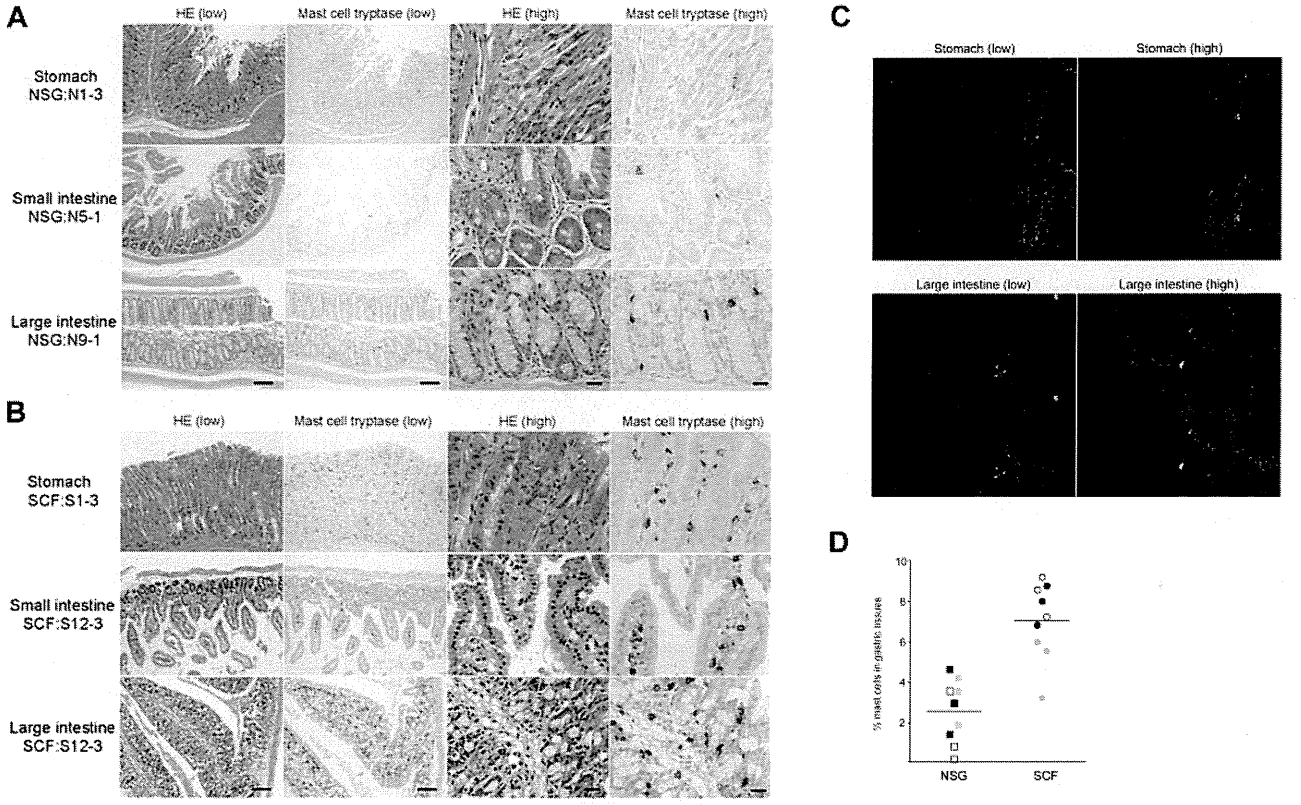

Figure 5. Human mast cell development in hSCF Tg NSG recipient stomach, small intestine, and large intestine. H&E- and anti–mast cell tryptase antibody–stained sections of (A) non-Tg NSG recipient stomach (NSG control, N1-3), small intestine (N5-1), and large intestine (N9-1) and (B) hSCF Tg NSG recipient stomach (S1-3), small intestine (S12-3), and large intestine (S12-3) demonstrating the presence of human mast cells (N1-3, killed at 24 weeks; N5-1, killed at 35 weeks; N9-1, killed at 20 weeks; S1-3, killed at 21 weeks; and S12-3, killed at 13 weeks). (C) Confocal immunofluorescence images of hSCF Tg stomach (S1-9) demonstrate human CD45$^+$ (green) and human CD117$^+$ (red) mast cells. (D) Frequencies of tryptase$^+$ cells were quantified by sampling 3 areas each from hSCF Tg (n = 3) and non-Tg (n = 3) NSG recipients: hSCF Tg NSG recipients, 7.0% ± 0.6%; and non-Tg NSG recipients, 2.5% ± 0.5% ($P < .0001$ by 2-tailed t test).

identify transcriptional signature specific to the immature human granulocytes that developed in the hSCF Tg NSG mice. Approximately 300 genes were differentially transcribed in the immature granulocytes in hSCF Tg NSG recipients compared with the mature granulocytes in non-Tg NSG recipients. Some of the up-regulated genes were associated with cell cycle or metabolism.

In several hSCF Tg NSG recipients, human mast cells composed the greatest subfraction among engrafted human myeloid cells. In the spleens of hSCF Tg NSG-engrafted mice, human mast cells were present at the highest frequency among the myeloid lineage developed in the recipients. MGG staining revealed both mature and immature mast cells in hSCF Tg NSG recipient BM. Human mast cells were identified not only in hematopoietic organs but also in lung, gastric tissue, and intestinal tissues of hSCF Tg NSG recipients. Aberrant expression of CD30 and CD25 on mast cells is associated with systemic mastocytosis and other mast cell disorders.[36,37] We did not find significantly up-regulated expression of these antigens in the mast cells derived from BM or spleen of hSCF Tg NSG recipients.

To date, several mouse strains have been developed for supporting normal and malignant human hematopoietic cell engraftment and normal myeloid cell differentiation using *Il2rg*^{null} immune-compromised mice (supplemental Table 3).[5,6,8,9,20,38-41] Among these, human thrombopoietin knock-in *Rag2*^{null} *Il2rg*^{null} mice were reported to support both human hematopoietic engraftment and myeloid differentiation in the BM. Both SCF and thrombopoietin exhibit species specificity between humans and mouse in supporting HSCs and myeloid cells in both species. These approaches focusing on the 2 distinct molecules based on the 2 immune-compromised mouse backgrounds will allow us to investigate human hematopoiesis and immunity from stem cells to myeloid progenitors to mature myeloid effecter cells in vivo. Altogether, the newly created hSCF Tg NSG mouse model engrafted with purified human HSCs will facilitate the in vivo understanding of human hematopoietic hierarchy and mast cell biology.

Acknowledgments

The authors thank David Williams for providing C3H/HeJ mice carrying the human SCF transgene and Dr Kodo and his staff at the Tokyo Cord Blood Bank for their generous assistance in processing and providing cord blood samples.

This work was supported by the National Institutes of Health (research grants HL077642, CA34196, AI46629, UO1 AI073871, DK089572), the University of Massachusetts Center for AIDS Research (P30 AI042845), the Juvenile Diabetes Foundation, International, the Helmsley Foundation, USAMRIID (L.D.S.), Project for Developing Innovation Systems, Program for Fostering Regional Innovation (O.O.), Takeda Science Foundation and Ministry of Education, Culture, Sports, Science and Technology, Japan (F.I.), and the Japan Society for the Promotion of Science through the Funding Program for Next Generation World-Leading Researchers (NEXT Program), initiated by the Council for Science and Technology Policy.

The contents of this publication are solely the responsibility of the authors and do not necessarily represent the official views of the National Institutes of Health.

Authorship

Contribution: S. Takagi, S. Tanaka, T.H., and S.M. performed the experiments; A.H., T.W., and O.O. performed and analyzed the microarray experiments; J.K., H. Kiyono, H. Koseki, O.O., T.S., and S. Taniguchi participated in discussions on research planning and analysis of results; and S. Takagi, Y.S., L.D.S., and F.I. designed the research and wrote the paper.

Conflict-of-interest disclosure: The authors declare no competing financial interests.

Correspondence: Fumihiko Ishikawa, Research Unit for Human Disease Models, RIKEN Research Center for Allergy and Immunology, 1-7-22 Suehiro-cho Tsurumi-ku, Yokohama, Kanagawa, Japan 230-0045; e-mail: f_ishika@rcai.riken.jp.

References

1. Manz MG. Human-hemato-lymphoid-system mice: opportunities and challenges. *Immunity.* 2007;26(5):537-541.
2. Shultz LD, Ishikawa F, Greiner DL. Humanized mice in translational biomedical research. *Nat Rev Immunol.* 2007;7(2):118-130.
3. McCune JM, Namikawa R, Kaneshima H, Shultz LD, Lieberman M, Weissman IL. The SCID-hu mouse: murine model for the analysis of human hematolymphoid differentiation and function. *Science.* 1988;241(4873):1632-1639.
4. Mosier DE, Gulizia RJ, Baird SM, Wilson DB. Transfer of a functional human immune system to mice with severe combined immunodeficiency. *Nature.* 1988;335(6187):256-259.
5. Ishikawa F, Yasukawa M, Lyons B, et al. Development of functional human blood and immune systems in NOD/SCID/IL2 receptor gamma chain-(null) mice. *Blood.* 2005;106(5):1565-1573.
6. Ito M, Hiramatsu H, Kobayashi K, et al. NOD/SCID/gamma(c)(null) mouse: an excellent recipient mouse model for engraftment of human cells. *Blood.* 2002;100(9):3175-3182.
7. Shultz LD, Banuelos S, Lyons B, et al. NOD/LtSz-Rag1nullPfpnull mice: a new model system with increased levels of human peripheral leukocyte and hematopoietic stem-cell engraftment. *Transplantation.* 2003;76(7):1036-1042.
8. Shultz LD, Lyons BL, Burzenski LM, et al. Human lymphoid and myeloid cell development in NOD/LtSz-scid IL2R gamma null mice engrafted with mobilized human hemopoietic stem cells. *J Immunol.* 2005;174(10):6477-6489.
9. Traggiai E, Chicha L, Mazzucchelli L, et al. Development of a human adaptive immune system in cord blood cell-transplanted mice. *Science.* 2004; 304(5667):104-107.
10. Strowig T, Gurer C, Ploss A, et al. Priming of protective T cell responses against virus-induced tumors in mice with human immune system components. *J Exp Med.* 2009;206(6):1423-1434.
11. Jaiswal S, Pearson T, Friberg H, et al. Dengue virus infection and virus-specific HLA-A2 restricted immune responses in humanized NOD-scid IL2rgammanull mice. *PLoS One.* 2009;4(10): e7251.
12. Shultz LD, Saito Y, Najima Y, et al. Generation of functional human T-cell subsets with HLA-restricted immune responses in HLA class I expressing NOD/SCID/IL2r gamma(null) humanized mice. *Proc Natl Acad Sci U S A.* 2010; 107(29):13022-13027.
13. Majumdar MK, Everett ET, Xiao X, et al. Xenogeneic expression of human stem cell factor in transgenic mice mimics codominant c-kit mutations. *Blood.* 1996;87(8):3203-3211.
14. Hong F, Breitling R, McEntee CW, et al. RankProd: a bioconductor package for detecting differentially expressed genes in meta-analysis. *Bioinformatics.* 2006;22(22):2825-2827.
15. Draghici S, Khatri P, Martins RP, et al. Global functional profiling of gene expression. *Genomics.* 2003;81(2):98-104.
16. Benjamini Y, Hochberg Y, et al. Controlling the false discovery rate: a practical and powerful approach to multiple testing. *J R Stat Soc B Met.* 1995;57(1):289-300.
17. Kawashima I, Zanjani ED, Almaida-Porada G, Flake AW, Zeng H, Ogawa M. CD34+ human marrow cells that express low levels of Kit protein are enriched for long-term marrow-engrafting cells. *Blood.* 1996;87(10):4136-4142.
18. Sakabe H, Kimura T, Zeng Z, et al. Haematopoietic action of flt3 ligand on cord blood-derived CD34-positive cells expressing different levels of flt3 or c-kit tyrosine kinase receptor: comparison with stem cell factor. *Eur J Haematol.* 1998;60(5): 297-306.
19. Yoshikubo T, Inoue T, Noguchi M, Okabe H. Differentiation and maintenance of mast cells from CD34+ human cord blood cells. *Exp Hematol.* 2006;34(3):320-329.
20. Hiramatsu H, Nishikomori R, Heike T, et al. Complete reconstitution of human lymphocytes from cord blood CD34+ cells using the NOD/SCID/gammacnull mice model. *Blood.* 2003;102(3): 873-880.
21. Arinobu Y, Iwasaki H, Gurish MF, et al. Developmental checkpoints of the basophil/mast cell lineages in adult murine hematopoiesis. *Proc Natl Acad Sci U S A.* 2005;102(50):18105-18110.
22. Kiel MJ, Morrison SJ. Uncertainty in the niches that maintain haematopoietic stem cells. *Nat Rev Immunol.* 2008;8(4):290-301.
23. Jenkinson EJ, Jenkinson WE, Rossi SW, Anderson G. The thymus and T-cell commitment: the right niche for Notch? *Nat Rev Immunol.* 2006;6(7):551-555.
24. Toksoz D, Zsebo KM, Smith KA, et al. Support of human hematopoiesis in long-term bone marrow cultures by murine stromal cells selectively expressing the membrane-bound and secreted forms of the human homolog of the steel gene product, stem cell factor. *Proc Natl Acad Sci U S A.* 1992;89(16):7350-7354.
25. Besmer P, Manova K, Duttlinger R, et al. The kit-ligand (steel factor) and its receptor c-kit/W: pleiotropic roles in gametogenesis and melanogenesis. *Dev Suppl.* 1993;125-137.
26. Geissler EN, McFarland EC, Russell ES. Analysis of pleiotropism at the dominant white-spotting (W) locus of the house mouse: a description of ten new W alleles. *Genetics.* 1981;97(2):337-361.
27. Russell ES. Hereditary anemias of the mouse: a review for geneticists. *Adv Genet.* 1979;20:357-459.
28. Broudy VC. Stem cell factor and hematopoiesis. *Blood.* 1997;90(4):1345-1364.
29. Leary AG, Zeng HQ, Clark SC, Ogawa M. Growth factor requirements for survival in G0 and entry into the cell cycle of primitive human hemopoietic progenitors. *Proc Natl Acad Sci U S A.* 1992; 89(9):4013-4017.
30. Bernstein ID, Andrews RG, Zsebo KM. Recombinant human stem cell factor enhances the formation of colonies by CD34+ and CD34+lin− cells, and the generation of colony-forming cell progeny from CD34+lin− cells cultured with interleukin-3, granulocyte colony-stimulating factor, or granulocyte-macrophage colony-stimulating factor. *Blood.* 1991;77(11):2316-2321.
31. Haylock DN, To LB, Dowse TL, Juttner CA, Simmons PJ. Ex vivo expansion and maturation of peripheral blood CD34+ cells into the myeloid lineage. *Blood.* 1992;80(6):1405-1412.
32. Petzer AL, Hogge DE, Landsdorp PM, Reid DS, Eaves CJ. Self-renewal of primitive human hematopoietic cells (long-term-culture-initiating cells) in vitro and their expansion in defined medium. *Proc Natl Acad Sci U S A.* 1996;93(4):1470-1474.
33. Lev S, Yarden Y, Givol D. Dimerization and activation of the kit receptor by monovalent and bivalent binding of the stem cell factor. *J Biol Chem.* 1992;267(22):15970-15977.
34. Martin FH, Suggs SV, Langley KE, et al. Primary structure and functional expression of rat and human stem cell factor DNAs. *Cell.* 1990;63(1):203-211.
35. Terstappen LW, Safford M, Loken MR. Flow cytometric analysis of human bone marrow: III. Neutrophil maturation. *Leukemia.* 1990;4(9):657-663.
36. Pardanani A. Systemic mastocytosis in adults: 2011 update on diagnosis, risk stratification, and management. *Am J Hematol.* 2011;86(4):362-371.
37. Sotlar K, Cerny-Reiterer S, Petat-Dutter K, et al. Aberrant expression of CD30 in neoplastic mast cells in high-grade mastocytosis. *Mod Pathol.* 2011;24(4):585-595.
38. Rongvaux A, Willinger T, Takizawa H, et al. Human thrombopoietin knockin mice efficiently support human hematopoiesis in vivo. *Proc Natl Acad Sci U S A.* 2011;108(6):2378-2383.
39. Pearson T, Shultz LD, Miller D, et al. Non-obese diabetic-recombination activating gene-1 (NOD-Rag1 null) interleukin (IL)-2 receptor common gamma chain (IL2r gamma null) null mice: a radioresistant model for human lymphohaematopoietic engraftment. *Clin Exp Immunol.* 2008;154(2): 270-284.
40. Brehm MA, Cuthbert A, Yang C, et al. Parameters for establishing humanized mouse models to study human immunity: analysis of human hematopoietic stem cell engraftment in three immunodeficient strains of mice bearing the IL2rgamma(null) mutation. *Clin Immunol.* 2010;135(1):84-98.
41. Strowig T, Rongvaux A, Rathinam C, et al. Transgenic expression of human signal regulatory protein alpha in Rag2−/−gammac−/− mice improves engraftment of human hematopoietic cells in humanized mice. *Proc Natl Acad Sci U S A.* 2011;108(32):13218-13223.